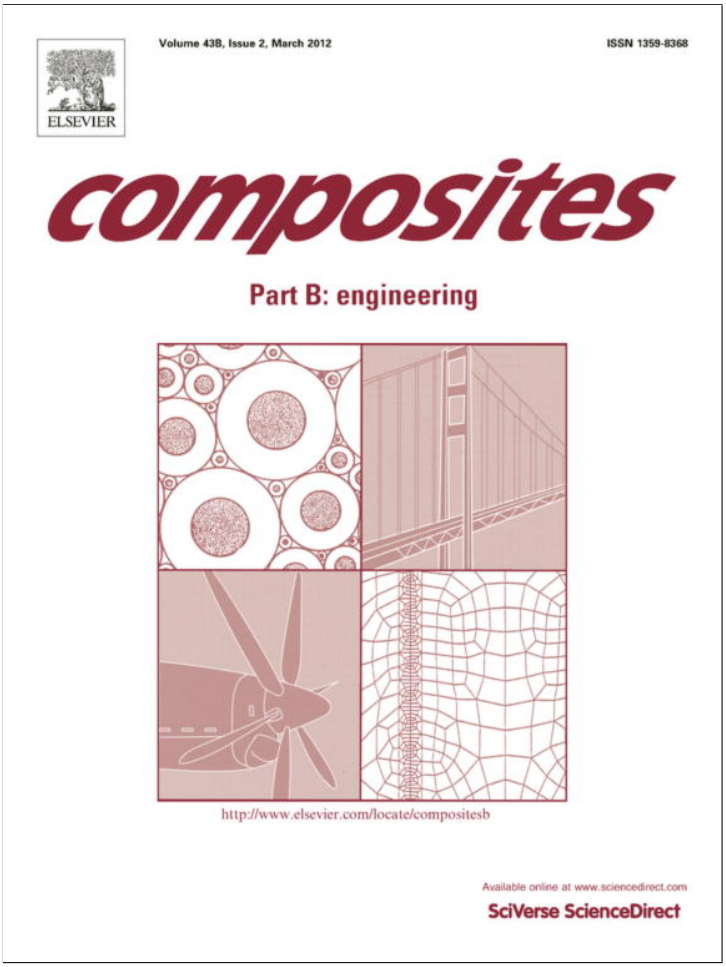

Composites: Part B 43 (2012) 711–725

Contents lists available at SciVerse ScienceDirect

Composites: Part B

journal homepage: www.elsevier.com/locate/compositesb

A quasi-3D sinusoidal shear deformation theory for the static and free vibration analysis of functionally graded plates

A.M.A. Neves [a], A.J.M. Ferreira [a,*], E. Carrera [c], C.M.C. Roque [b], M. Cinefra [c], R.M.N. Jorge [a], C.M.M. Soares [d]

[a] Departamento de Engenharia Mecânica, Faculdade de Engenharia, Universidade do Porto, Rua Dr. Roberto Frias, 4200-465 Porto, Portugal
[b] INEGI, Faculdade de Engenharia, Universidade do Porto, Rua Dr. Roberto Frias, 4200-465 Porto, Portugal
[c] Departament of Aeronautics and Aerospace Engineering, Politecnico di Torino, Corso Duca degli Abruzzi, 24, 10129 Torino, Italy
[d] Instituto Superior Técnico, Av. Rovisco Pais, Lisboa, Portugal

ARTICLE INFO

Article history:
Received 16 July 2011
Accepted 14 August 2011
Available online 25 August 2011

Keywords:
A. Layered structures
C. Computational modelling

ABSTRACT

In this paper we present a new application for Carrera's unified Formulation (CUF) to analyse functionally graded plates.

In this paper the authors present explicit governing equations of a sinusoidal shear deformation theory for functionally graded plates. It addresses the bending and free vibration analysis and accounts for through-the-thickness deformations.

The equations of motion are interpolated by collocation with radial basis functions. Numerical examples demonstrate the efficiency of the present approach.

1. Introduction

Functionally graded materials (FGM) are a class of composites in which the properties of the material gradually change over one or more cartesian direction. A typical FGM plate considers a continuous variation of material properties over the thickness direction by mixing two different materials [1]. The gradual variation of properties avoids the delamination failure that are common in laminated composites. The FGM concept has applications in several fields such as aerospace and civil [1]. The increase of FGM applications requires accurate plate theories. Typically, the analysis of FGM plates is performed using the first-order shear deformation theory (FSDT) [2–5] or higher-order shear deformation theories (HSDT) [3,5–8]. The FSDT gives acceptable results but depends on the shear correction factor which is hard to find as it depends on many parameters. There is no need of a shear correction factor when using a HSDT but equations of motion are more complicated than those of the FSDT. Carrera's Unified Formulation (CUF) made the implementation of such theories easier.

Typically functionally graded plates have been analysed with shear deformation theories that neglect the thickness stretching ϵ_{zz}, being the transverse displacement considered to be independent of thickness coordinates. The effect of thickness stretching in FGM plates has been recently investigated by Carrera et al. [9], using finite element approximations.

The use of alternative methods to the finite element methods for the analysis of plates, such as the meshless methods based on collocation with radial basis functions is atractive due to the absence of a mesh and the ease of collocation methods. In recent years, radial basis functions (RBFs) showed excellent accuracy in the interpolation of data and functions. Kansa [10] introduced the concept of solving partial differential equations by an unsymmetric RBF collocation method based upon the multiquadric interpolation functions. The authors have recently applied the RBF collocation to the static deformations and free vibrations of composite beams and plates [11–18].

The present paper addresses the thickness stretching issue on the static and free vibration analysis of FGM plates, by a meshless technique based on collocation with radial basis functions. The CUF method [19,20] is employed to obtain the algebraic equations of motion and boundary conditions. Such equations of motion and corresponding boundary conditions are then interpolated by radial basis functions to obtain an algebraic system of equations.

2. Governing equations and boundary conditions in the framework of unified formulation

The unified formulation proposed by Carrera [19,20] (further denoted as CUF) has been applied in several finite element analysis, either using the Principle of Virtual Displacements, or by using the Reissner's Mixed Variational theorem. The stiffness matrix components, the external force terms or the inertia terms can be obtained directly with this unified formulation, irrespective of the shear deformation theory being considered.

* Corresponding author.
E-mail address: ferreira@fe.up.pt (A.J.M. Ferreira).

1359-8368/$ - see front matter © 2011 Elsevier Ltd. All rights reserved.
doi:10.1016/j.compositesb.2011.08.009

For the sake of completeness, the meshless version of Carrera's unified formulation [19,20] is briefly reviewed. It is shown how to obtain the fundamental nuclei, which allows the derivation of the equations of motion and boundary conditions, for the present collocation with RBFs.

The use of sinusoidal shear deformation plate theory was first presented by Touratier [21–23], later by Vidal and Polit [24], and recently by Neves et al. [25]. The use of sinusoidal plate theories for functionally graded plates was presented by Zenkour [2], where a $\epsilon_{zz} = 0$ approach was used. The use of trigonometric shear deformation theory accounting for $\epsilon_{zz} \neq 0$ for the analysis of plates has not been used before. In this paper we consider an hybrid quasi-3D sinusoidal shear deformation theory, with different expansion for the in-plane displacements (u, v) and the out-of-plane displacement (w).

Consider a rectangular plate of plan-form dimensions a and b and uniform thickness h. The co-ordinate system is taken such that the x–y plane coincides with the midplane of the plate. The plate is composed of a functionally graded material across the thickness direction.

2.1. Displacement field

A generalization of the CUF concepts is introduced here by considering different expansions for every displacement component as function of the thickness variable. In-plane displacements are considered to be of sinusoidal type across the thickness coordinate,

$$u = u_0 + zu_1 + \sin\left(\frac{\pi z}{h}\right)u_Z \tag{1}$$

$$v = v_0 + zv_1 + \sin\left(\frac{\pi z}{h}\right)v_Z \tag{2}$$

while the transverse displacement is defined as quadratic in the thickness direction

$$w = w_0 + zw_1 + z^2 w_Z \tag{3}$$

It turns out that the present formulation can be seen as a generalization of the original CUF, by introducing different displacement fields for in-plane and out-of-plane displacements.

2.2. Strains

Stresses and strains are separated into in-plane and normal components, denoted respectively by the subscripts p and n. The mechanical strains in the kth layer can be related to the displacement field $\mathbf{u}^k = \left\{u_x^k, u_y^k, u_z^k\right\}$ via the geometrical relations:

$$\begin{aligned} \epsilon_{pG}^k &= \left[\epsilon_{xx}, \epsilon_{yy}, \gamma_{xy}\right]^{kT} = \mathbf{D}_p^k \mathbf{u}^k \\ \epsilon_{nG}^k &= \left[\gamma_{xz}, \gamma_{yz}, \epsilon_{zz}\right]^{kT} = \left(\mathbf{D}_{np}^k + \mathbf{D}_{nz}^k\right)\mathbf{u}^k \end{aligned} \tag{4}$$

wherein the differential operator arrays are defined as follows:

$$\mathbf{D}_p^k = \begin{bmatrix} \partial_x & 0 & 0 \\ 0 & \partial_y & 0 \\ \partial_y & \partial_x & 0 \end{bmatrix} \quad \mathbf{D}_{np}^k = \begin{bmatrix} 0 & 0 & \partial_x \\ 0 & 0 & \partial_y \\ 0 & 0 & 0 \end{bmatrix} \quad \mathbf{D}_{nz}^k = \begin{bmatrix} \partial_z & 0 & 0 \\ 0 & \partial_z & 0 \\ 0 & 0 & \partial_z \end{bmatrix} \tag{5}$$

2.3. Elastic stress–strain relations

The 3D constitutive equations in each layer k are given as:

$$\begin{aligned} \sigma_{pC}^k &= \mathbf{C}_{pp}^k \epsilon_{pG}^k + \mathbf{C}_{pn}^k \epsilon_{nG}^k \\ \sigma_{nC}^k &= \mathbf{C}_{np}^k \epsilon_{pG}^k + \mathbf{C}_{nn}^k \epsilon_{nG}^k \end{aligned} \tag{6}$$

with

$$\begin{aligned} \mathbf{C}_{pp}^k &= \begin{bmatrix} C_{11} & C_{12} & 0 \\ C_{12} & C_{22} & 0 \\ 0 & 0 & C_{66} \end{bmatrix} \quad \mathbf{C}_{pn}^k = \begin{bmatrix} 0 & 0 & C_{13} \\ 0 & 0 & C_{23} \\ 0 & 0 & 0 \end{bmatrix} \\ \mathbf{C}_{np}^k &= \begin{bmatrix} 0 & 0 & 0 \\ 0 & 0 & 0 \\ C_{13} & C_{23} & 0 \end{bmatrix} \quad \mathbf{C}_{nn}^k = \begin{bmatrix} C_{55} & 0 & 0 \\ 0 & C_{44} & 0 \\ 0 & 0 & C_{33} \end{bmatrix} \end{aligned} \tag{7}$$

The functionally graded plate is divided into a number of uniform thickness layers. For every layer, we define the volume fraction of the ceramic phase as:

$$V_c = \left(0.5 + \frac{z}{h}\right)^p \tag{8}$$

where $z \in [-h/2, h/2]$, and p is a scalar parameter that allows the user to define gradation of material properties across the thickness direction. The volume fraction for the metal phase is given as $V_m = 1 - V_c$.

The computation of the elastic constants C_{ij}^k depends on which assumption of ϵ_{zz} we consider. If $\epsilon_{zz} = 0$, then C_{ij}^k are the plane-stress reduced elastic constants:

$$C_{11}^k = \frac{E^k}{1-(\nu^k)^2}, \quad C_{12}^k = \nu^k \frac{E^k}{1-(\nu^k)^2}, \quad C_{22}^k = \frac{E^k}{1-(\nu^k)^2} \tag{9}$$

$$C_{44}^k = G^k, \quad C_{55}^k = G^k, \quad C_{66}^k = G^k, \quad C_{33}^k = 0 \tag{10}$$

where E^k is the modulus of elasticity, ν^k is the Poisson's ratio, and G^k is the shear modulus $G^k = \frac{E^k}{2(1+\nu^k)}$ for each layer.

It is interesting to note that the present theory does not consider the use of shear-correction factors, as would be the case of the first-order shear deformation theory (FSDT).

If $\epsilon_{zz} \neq 0$ (thickness stretching), then C_{ij}^k are the three-dimensional elastic constants, given by

$$C_{11}^k = \frac{E^k(1-(\nu^k)^2)}{1-3(\nu^k)^2-2(\nu^k)^3}, \quad C_{12}^k = \frac{E^k(\nu^k+(\nu^k)^2)}{1-3(\nu^k)^2-2(\nu^k)^3}, \quad C_{22}^k = \frac{E^k(1-(\nu^k)^2)}{1-3(\nu^k)^2-2(\nu^k)^3} \tag{11}$$

$$C_{44}^k = G^k, \quad C_{55}^k = G^k, \quad C_{66}^k = G^k, \quad C_{33}^k = \frac{E^k(1-(\nu^k)^2)}{1-3(\nu^k)^2-2(\nu^k)^3} \tag{12}$$

In the CUF formulation we consider virtual (mathematical) layers of constant thickness, each containing a homogeneized modulus of elasticity, E^k, and a homogeneized Poisson's ratio, ν^k.

For each virtual layer, the elastic properties E^k and ν^k can be computed in two ways. First, we may consider the the law-of-mistures:

$$E^k(z) = E_m V_m + E_c V_c \quad \nu^k(z) = \nu_m V_m + \nu_c V_c \tag{13}$$

Second, and perhaps more interesting, we may consider the Mori–Tanaka homogenization procedure. In this homogenization method, we find the bulk modulus, K, and the effective shear modulus, G, of the composite equivalent layer as

$$\frac{K-K_1}{K_2-K_1} = \frac{V_2}{1+(1-V_2)\frac{K_2-K_1}{K_1+4/3G_1}} \quad \frac{G-G_1}{G_2-G_1} = \frac{V_2}{1+(1-V_2)\frac{G_2-G_1}{G_1+f_1}} \tag{14}$$

where

$$f_1 = \frac{G_1(9K_1+8G_1)}{6(K_1+2G_1)} \tag{15}$$

The effective values of Young's modulus, E^k, and Poisson's ratio, ν^k, are found from

$$E^k = \frac{9KG}{3K+G}; \quad \nu^k = \frac{3K-2G}{2(3K+G)} \tag{16}$$

2.4. Governing equations

The three displacement components u_x, u_y and u_z (given in (1)–(3)) and their relative variations can be modelled as:

$$\begin{aligned}(u_x,u_y,u_z) &= F_\tau(u_{x\tau},u_{y\tau},u_{z\tau}) \quad (\delta u_x,\delta u_y,\delta u_z)\\ &= F_s(\delta u_{xs},\delta u_{ys},\delta u_{zs})\end{aligned} \tag{17}$$

In the present formulation the thickness functions are

$$F_{sux}=F_{suy}=F_{\tau ux}=F_{\tau uy}=\left[1 \quad z \quad \sin\left(\frac{\pi z}{h}\right)\right] \tag{18}$$

for inplane displacements u, v and

$$F_{suz}=F_{\tau uz}=[1 \quad z \quad z^2] \tag{19}$$

for transverse displacement w. We then obtain all terms of the equations of motion by integrating through the thickness direction.

It is interesting to note that under this combination of the unified formulation and RBF collocation, the collocation code depends only on the choice of F_τ, F_s, in order to solve this type of problems. We designed a MATLAB code that just by changing F_τ, F_s can analyse static deformations and free vibrations for any type of C_z^0 shear deformation theory.

A multi-layered functionally graded plate with N_l layers is considered. The Principle of Virtual Displacements (PVD) for the mechanical case is defined as:

$$\sum_{k=1}^{N_l}\int_{\Omega_k}\int_{A_k}\left\{\delta\epsilon_{pG}^{k\,T}\sigma_{pC}^k+\delta\epsilon_{nG}^{k\,T}\sigma_{nC}^k\right\}d\Omega_k\,dz=\sum_{k=1}^{N_l}\delta L_e^k \tag{20}$$

where Ω_k and A_k are the integration domains in plane (x,y) and z direction, respectively. Here, k indicates the layer and T the transpose of a vector, and δL_e^k is the external work for the kth layer. G means geometrical relations and C constitutive equations.

Substituting the geometrical relations, the constitutive equations and the unified formulation into the variational statement PVD, for the kth layer, one has:

$$\begin{aligned}&\int_{\Omega_k}\int_{A_k}\left[\left(\mathbf{D}_p^k F_s\delta\mathbf{u}_s^k\right)^T\left(\mathbf{C}_{pp}^k\mathbf{D}_p^k F_\tau\mathbf{u}_\tau^k+\mathbf{C}_{pn}^k\left(\mathbf{D}_{n\Omega}^k+\mathbf{D}_{nz}^k\right)F_\tau\mathbf{u}_\tau^k\right)\right.\\ &\left.+\left(\left(\mathbf{D}_{n\Omega}^k+\mathbf{D}_{nz}^k\right)F_s\delta\mathbf{u}_s^k\right)^T\left(\mathbf{C}_{np}^k\mathbf{D}_p^k F_\tau\mathbf{u}_\tau^k+\mathbf{C}_{nn}^k\left(\mathbf{D}_{n\Omega}^k+\mathbf{D}_{nz}^k\right)F_\tau\mathbf{u}_\tau^k\right)\right]d\Omega_k\,dz=\delta L_e^k\end{aligned} \tag{21}$$

At this point, the formula of integration by parts is applied:

$$\int_{\Omega_k}((\mathbf{D}_\Omega)\delta\mathbf{a}^k)^T\mathbf{a}^k\,d\Omega_k=-\int_{\Omega_k}\delta\mathbf{a}^{k\,T}((\mathbf{D}_\Omega^T)\mathbf{a}^k)d\Omega_k+\int_{\Gamma_k}\delta\mathbf{a}^{k\,T}((\mathbf{I}_\Omega)\mathbf{a}^k)d\Gamma_k \tag{22}$$

where $\mathbf{I}_\Omega$ matrix is obtained applying the *Gradient theorem*:

$$\int_\Omega\frac{\partial\psi}{\partial x_i}d\upsilon=\oint_\Gamma n_i\psi\,ds \tag{23}$$

being n_i the components of the normal $\hat{n}$ to the boundary along the direction i. After integration by parts, the governing equations and boundary conditions for the plate in the mechanical case are obtained:

$$\begin{aligned}&\int_{\Omega_k}\int_{A_k}\left(\delta\mathbf{u}_s^k\right)^T\left[\left(\left(-\mathbf{D}_p^k\right)^T\left(\mathbf{C}_{pp}^k(\mathbf{D}_p^k)+\mathbf{C}_{pn}^k\left(\mathbf{D}_{n\Omega}^k+\mathbf{D}_{nz}^k\right)\right)\right.\right.\\ &\left.+\left(-\mathbf{D}_{n\Omega}^k+\mathbf{D}_{nz}^k\right)^T\left(\mathbf{C}_{np}^k(\mathbf{D}_p^k)+\mathbf{C}_{nn}^k(\mathbf{D}_{n\Omega}^k+\mathbf{D}_{nz}^k)\right)\right)F_\tau F_s\mathbf{u}_\tau^k\Big]dx\,dy\,dz\\ &+\int_{\Omega_k}\int_{A_k}\left(\delta\mathbf{u}_s^k\right)^T\left[\left(\mathbf{I}_p^{kT}\left(\mathbf{C}_{pp}^k(\mathbf{D}_p^k)+\mathbf{C}_{pn}^k(\mathbf{D}_{n\Omega}^k+\mathbf{D}_{nz}^k)\right)\right.\right.\\ &\left.\left.+\mathbf{I}_{np}^{kT}\left(\mathbf{C}_{np}^k(\mathbf{D}_p^k)+\mathbf{C}_{nn}^k(\mathbf{D}_{n\Omega}^k+\mathbf{D}_{nz}^k)\right)\right)F_\tau F_s\mathbf{u}_\tau^k\Big]dx\,dy\,dz\\ &=\int_{\Omega_k}\delta\mathbf{u}_s^{kT}F_s\mathbf{p}^k\,d\Omega_k\end{aligned} \tag{24}$$

where $\mathbf{I}_p^k$ and $\mathbf{I}_{np}^k$ depend on the boundary geometry:

$$\mathbf{I}_p^k=\begin{bmatrix}n_x&0&0\\0&n_y&0\\n_y&n_x&0\end{bmatrix}\quad\mathbf{I}_{np}^k=\begin{bmatrix}0&0&n_x\\0&0&n_y\\0&0&0\end{bmatrix} \tag{25}$$

The normal to the boundary of domain Ω is:

$$\hat{\mathbf{n}}=\begin{bmatrix}n_x\\n_y\end{bmatrix}=\begin{bmatrix}cos(\varphi_x)\\cos(\varphi_y)\end{bmatrix} \tag{26}$$

where φ_x and φ_y are the angles between the normal $\hat{n}$ and the direction x and y respectively.

The governing equations for a multi-layered plate subjected to mechanical loadings are:

$$\delta\mathbf{u}_s^{k\,T}:\mathbf{K}_{uu}^{k\tau s}\mathbf{u}_\tau^k=\mathbf{P}_{u\tau}^k \tag{27}$$

where the fundamental nucleus $\mathbf{K}_{uu}^{k\tau s}$ is obtained as:

$$\begin{aligned}\mathbf{K}_{uu}^{k\tau s}=&\left[\left(-\mathbf{D}_p^k\right)^T\left(\mathbf{C}_{pp}^k(\mathbf{D}_p^k)+\mathbf{C}_{pn}^k(\mathbf{D}_{n\Omega}^k+\mathbf{D}_{nz}^k)\right)\right.\\ &\left.+\left(-\mathbf{D}_{n\Omega}^k+\mathbf{D}_{nz}^k\right)^T\left(\mathbf{C}_{np}^k(\mathbf{D}_p^k)+\mathbf{C}_{nn}^k(\mathbf{D}_{n\Omega}^k+\mathbf{D}_{nz}^k)\right)\right]F_\tau F_s\end{aligned} \tag{28}$$

and the corresponding Neumann-type boundary conditions on Γ_k are:

$$\mathbf{\Pi}_d^{k\tau s}\mathbf{u}_\tau^k=\mathbf{\Pi}_d^{k\tau s}\bar{\mathbf{u}}_\tau^k \tag{29}$$

where

$$\begin{aligned}\mathbf{\Pi}_d^{k\tau s}=&\left[\mathbf{I}_p^{kT}\left(\mathbf{C}_{pp}^k\left(\mathbf{D}_p^k\right)+\mathbf{C}_{pn}^k(\mathbf{D}_{n\Omega}^k+\mathbf{D}_{nz}^k)\right)+\mathbf{I}_{np}^{kT}\left(\mathbf{C}_{np}^k\left(\mathbf{D}_p^k\right)\right.\right.\\ &\left.\left.+\mathbf{C}_{nn}^k\left(\mathbf{D}_{n\Omega}^k+\mathbf{D}_{nz}^k\right)\right)\right]F_\tau F_s\end{aligned} \tag{30}$$

and $\mathbf{P}_{u\tau}^k$ are variationally consistent loads with applied pressure.

2.5. Dynamic governing equations

The PVD for the dynamic case is expressed as:

$$\begin{aligned}&\sum_{k=1}^{N_l}\int_{\Omega_k}\int_{A_k}\left\{\delta\epsilon_{pG}^{k\,T}\sigma_{pC}^k+\delta\epsilon_{nG}^{k\,T}\sigma_{nC}^k\right\}d\Omega_k\,dz\\ &=\sum_{k=1}^{N_l}\int_{\Omega_k}\int_{A_k}\rho^k\delta\mathbf{u}^{kT}\ddot{\mathbf{u}}^k d\Omega_k\,dz+\sum_{k=1}^{N_l}\delta L_e^k\end{aligned} \tag{31}$$

where ρ^k is the mass density of the k-th layer and double dots denote acceleration.

By substituting the geometrical relations, the constitutive equations and the unified formulation, we obtain the following governing equations:

$$\delta\mathbf{u}_s^{k\,T}:\mathbf{K}_{uu}^{k\tau s}\mathbf{u}_\tau^k=\mathbf{M}^{k\tau s}\ddot{\mathbf{u}}_\tau^k+\mathbf{P}_{u\tau}^k \tag{32}$$

In the case of free vibrations one has:

$$\delta\mathbf{u}_s^{k\,T}:\mathbf{K}_{uu}^{k\tau s}\mathbf{u}_\tau^k=\mathbf{M}^{k\tau s}\ddot{\mathbf{u}}_\tau^k \tag{33}$$

where $\mathbf{M}^{k\tau s}$ is the fundamental nucleus for the inertial term. The explicit form of the inertial terms is

$$\begin{aligned}&M_{ij}^{k\tau s}=\sum_{k=1}^{N_l}\int_{z_k}^{z_{k+1}}\rho^k F_\tau F_s\,dz,\quad i=j=1,2,3\\ &M_{ij}^{k\tau s}=0,\quad i\neq j\end{aligned} \tag{34}$$

The geometrical and mechanical boundary conditions are the same of the static case.

2.6. Equations of motion and boundary conditions in terms of resultants

The following stress layer-resultants are defined:

$$\left(\boldsymbol{R}_p^{ks}, \boldsymbol{R}_n^{ks}\right) = \int_{A_k} \left(F_s \boldsymbol{\sigma}_p^k, F_s \boldsymbol{\sigma}_n^k\right) dz \tag{35}$$

where $\boldsymbol{R}_p^{ks} = \left\{R_{xx}^{ks}, R_{yy}^{ks}, R_{xy}^{ks}\right\}$ and $\boldsymbol{R}_n^{ks} = \left\{R_{xz}^{ks}, R_{yz}^{ks}, R_{zz}^{ks}\right\}$.

Substituting in (31), that includes the inertial term, and performing the integration by parts, one obtains:

$$\begin{aligned}
&\sum_{k=1}^{N_l} \left(\int_{\Omega^k} \delta \boldsymbol{u}_s^{kT} \left(-\boldsymbol{D}_p^{sT} \boldsymbol{R}_p^{ks} + \left(-\boldsymbol{D}_{n\Omega}^s + \boldsymbol{D}_{nz}^s\right)^T \boldsymbol{R}_n^{ks} \right) d\Omega^k \right. \\
&\left. + \int_{\Gamma^k} \delta \boldsymbol{u}_s^{kT} \left(\boldsymbol{I}_p^T \boldsymbol{R}_p^{ks} + \boldsymbol{I}_{np}^T \boldsymbol{R}_n^{ks} \right) d\Gamma^k \right) \\
&= \sum_{k=1}^{N_l} \int_{\Omega^k} \delta \boldsymbol{u}_s^{kT} \left(\rho^k E_{\tau s} \boldsymbol{I} \ddot{\boldsymbol{u}}_\tau^k + \boldsymbol{p}_s^k \right) d\Omega^k
\end{aligned} \tag{36}$$

where $E_{\tau s} = \int_{A^k} F_\tau F_s \, dz$ and $\boldsymbol{I}$ is the identity matrix.

By imposing the definition of virtual variations for the unknown displacements, the differential system of governing equations and related boundary conditions are derived in terms of the introduced stress resultants. For the k-layer, the equilibrium equations on Ω^k are:

$$\delta \boldsymbol{u}_s^{kT} : -\boldsymbol{D}_p^{sT} \boldsymbol{R}_p^{ks} + \left(-\boldsymbol{D}_{n\Omega}^s + \boldsymbol{D}_{nz}^s\right)^T \boldsymbol{R}_n^{ks} = E_{\tau s} \boldsymbol{I} \ddot{\boldsymbol{u}}_\tau^k + \boldsymbol{p}_s^k \tag{37}$$

while the boundary conditions on Γ^k are:

$$\boldsymbol{u}_s^k = \bar{\boldsymbol{u}}_s^k \quad \text{geometrical} \tag{38}$$

$$\boldsymbol{I}_p^T \boldsymbol{R}_p^{ks} + \boldsymbol{I}_{np}^T \boldsymbol{R}_n^{ks} = \boldsymbol{I}_p^T \overline{\boldsymbol{R}}_p^{ks} + \boldsymbol{I}_{np}^T \overline{\boldsymbol{R}}_n^{ks} \quad \text{mechanical} \tag{39}$$

We rename the resultants as follows:

$$\begin{aligned}
&\boldsymbol{R}_{xx}^0 = \int_A 1 \cdot \boldsymbol{\sigma}_{xx} = N_{xx}; \quad \boldsymbol{R}_{yy}^0 = N_{yy}; \quad \boldsymbol{R}_{xy}^0 = N_{xy} \\
&\boldsymbol{R}_{xz}^0 = Q_{xz}; \quad \boldsymbol{R}_{yz}^0 = Q_{yz}; \quad \boldsymbol{R}_{zz}^0 = Q_{zz} \quad (\text{for } s = 0)
\end{aligned} \tag{40}$$

$$\begin{aligned}
&\boldsymbol{R}_{xx}^1 = M_{xx}; \quad \boldsymbol{R}_{yy}^1 = M_{yy}; \quad \boldsymbol{R}_{xy}^1 = M_{xy} \\
&\boldsymbol{R}_{xz}^1 = M_{xz}; \quad \boldsymbol{R}_{yz}^1 = M_{yz}; \quad \boldsymbol{R}_{zz}^1 = M_{zz} \quad (\text{for } s = 1)
\end{aligned} \tag{41}$$

The name of resultants does not change for $s = Z$.

Substituting in the equilibrium Eqs. (37) and performing the products, one obtains the following equations of motion:

$$\begin{aligned}
\delta \boldsymbol{u}_0 &: -\partial_x N_{xx} - \partial_y N_{xy} + \partial_z Q_{xz} \\
&= \sum_{k=1}^{N_l} \int_{A_k} \rho^k (\ddot{u}_0 + z\ddot{u}_1 + \sin(z)\ddot{u}_Z) dz + (p_x + z p_x + \sin(z) p_x) \\
\delta \boldsymbol{v}_0 &: -\partial_x N_{xy} - \partial_y N_{yy} + \partial_z Q_{yz} \\
&= \sum_{k=1}^{N_l} \int_{A_k} \rho^k (\ddot{v}_0 + z\ddot{v}_1 + \sin(z)\ddot{v}_Z) dz + (p_y + z p_y + \sin(z) p_y) \\
\delta \boldsymbol{w}_0 &: -\partial_x Q_{xz} - \partial_y Q_{yz} + \partial_z Q_{zz} \\
&= \sum_{k=1}^{N_l} \int_{A_k} \rho^k (\ddot{w}_0 + z\ddot{w}_1 + z^2\ddot{w}_Z) dz + (p_z + z p_z + z^2 p_z) \\
\delta \boldsymbol{u}_1 &: -\partial_x M_{xx} - \partial_y M_{xy} + \partial_z M_{xz} \\
&= \sum_{k=1}^{N_l} \int_{A_k} \rho^k z (\ddot{u}_0 + z\ddot{u}_1 + \sin(z)\ddot{u}_Z) dz + (p_x + z p_x + \sin(z) p_x) \\
\delta \boldsymbol{v}_1 &: -\partial_x M_{xy} - \partial_y M_{yy} + \partial_z M_{yz} \\
&= \sum_{k=1}^{N_l} \int_{A_k} \rho^k z (\ddot{v}_0 + z\ddot{v}_1 + \sin(z)\ddot{v}_Z) dz + (p_y + z p_y + \sin(z) p_y) \\
\delta \boldsymbol{w}_1 &: -\partial_x M_{xz} - \partial_y M_{yz} + \partial_z M_{zz} \\
&= \sum_{k=1}^{N_l} \int_{A_k} \rho^k z (\ddot{w}_0 + z\ddot{w}_1 + z^2\ddot{w}_Z) dz + (p_z + z p_z + z^2 p_z) \\
\boldsymbol{u}_Z &: -\partial_x R_{xx}^Z - \partial_y R_{xy}^Z + \partial_z R_{xz}^Z \\
&= \sum_{k=1}^{N_l} \int_{A_k} \rho^k \sin(z) (\ddot{u}_0 + z\ddot{u}_1 + \sin(z)\ddot{u}_Z) dz + (p_x + z p_x + \sin(z) p_x) \\
\delta \boldsymbol{v}_Z &: -\partial_x R_{xy}^Z - \partial_y R_{yy}^Z + \partial_z R_{yz}^Z \\
&= \sum_{k=1}^{N_l} \int_{A_k} \rho^k \sin(z) (\ddot{v}_0 + z\ddot{v}_1 + \sin(z)\ddot{v}_Z) dz + (p_y + z p_y + \sin(z) p_y) \\
\delta \boldsymbol{w}_Z &: -\partial_x R_{xz}^Z - \partial_y R_{yz}^Z + \partial_z R_{zz}^Z \\
&= \sum_{k=1}^{N_l} \int_{A_k} \rho^k z^2 (\ddot{w}_0 + z\ddot{w}_1 + z^2\ddot{w}_Z) dz + (p_z + z p_z + z^2 p_z)
\end{aligned} \tag{42}$$

and the mechanical boundary conditions:

$$\begin{aligned}
&\delta \boldsymbol{u}_0 : n_x N_{xx} + n_y N_{xy} = n_x \overline{N}_{xx} + n_y \overline{N}_{xy} \\
&\delta \boldsymbol{v}_0 : n_x N_{xy} + n_y N_{yy} = n_x \overline{N}_{xy} + n_y \overline{N}_{yy} \\
&\delta \boldsymbol{w}_0 : n_x Q_{xz} + n_y Q_{yz} = n_x \overline{Q}_{xz} + n_y \overline{Q}_{yz} \\
&\delta \boldsymbol{u}_1 : n_x M_{xx} + n_y M_{xy} = n_x \overline{M}_{xx} + n_y \overline{M}_{xy} \\
&\delta \boldsymbol{v}_1 : n_x M_{xy} + n_y M_{yy} = n_x \overline{M}_{xy} + n_y \overline{M}_{yy} \\
&\delta \boldsymbol{w}_1 : n_x M_{xz} + n_y M_{yz} = n_x \overline{M}_{xz} + n_y \overline{M}_{yz} \\
&\delta \boldsymbol{u}_Z : n_x R_{xx}^Z + n_y R_{xy}^Z = n_x \overline{R}_{xx}^Z + n_y \overline{R}_{xy}^Z \\
&\delta \boldsymbol{v}_Z : n_x R_{xy}^Z + n_y R_{yy}^Z = n_x \overline{R}_{xy}^Z + n_y \overline{R}_{yy}^Z \\
&\delta \boldsymbol{w}_Z : n_x R_{xz}^Z + n_y R_{yz}^Z = n_x \overline{R}_{xz}^Z + n_y \overline{R}_{yz}^Z
\end{aligned} \tag{43}$$

2.7. Equations of motion and boundary conditions in terms of displacements

In order to discretize the equations of motion by radial basis functions, we present in the following the explicit terms of the equations of motion and the boundary conditions in terms of the generalized displacements.

$$\begin{aligned}
\delta u_0 : &-A_{11}\frac{\partial^2 u_0}{\partial x^2} - A_{66}\frac{\partial^2 u_0}{\partial y^2} - B_{11}\frac{\partial^2 u_1}{\partial x^2} - B_{66}\frac{\partial^2 u_1}{\partial y^2} + G_{11}\frac{\partial^2 u_Z}{\partial x^2} \\
&+ G_{66}\frac{\partial^2 u_Z}{\partial y^2} - (A_{12} + A_{66})\frac{\partial^2 v_0}{\partial x \partial y} - (B_{12} + B_{66})\frac{\partial^2 v_1}{\partial x \partial y} \\
&+ (G_{12} + G_{66})\frac{\partial^2 v_Z}{\partial x \partial y} + A_{55}\frac{\partial w_1}{\partial x} + H_{55}\frac{\partial w_Z}{\partial x} = I_0 \ddot{u}_0 + I_1 \ddot{u}_1 + I_5 \ddot{u}_Z
\end{aligned} \tag{44}$$

$$\begin{aligned}
\delta v_0 : &-(A_{12} + A_{66})\frac{\partial^2 u_0}{\partial x \partial y} - (B_{12} + B_{66})\frac{\partial^2 u_1}{\partial x \partial y} + (G_{12} + G_{66})\frac{\partial^2 u_Z}{\partial x \partial y} \\
&- A_{22}\frac{\partial^2 v_0}{\partial y^2} - A_{66}\frac{\partial^2 v_0}{\partial x^2} - B_{22}\frac{\partial^2 v_1}{\partial y^2} - B_{66}\frac{\partial^2 v_1}{\partial x^2} + G_{22}\frac{\partial^2 v_Z}{\partial y^2} \\
&+ G_{66}\frac{\partial^2 v_Z}{\partial x^2} + A_{44}\frac{\partial w_1}{\partial y} + H_{44}\frac{\partial w_Z}{\partial y} = I_0 \ddot{v}_0 + I_1 \ddot{v}_1 + I_5 \ddot{v}_Z
\end{aligned} \tag{45}$$

$$\begin{aligned}
\delta w_0 : &A_{13}\frac{\partial u_1}{\partial x} + 2B_{13}\frac{\partial u_Z}{\partial x} + A_{23}\frac{\partial v_1}{\partial y} + 2B_{23}\frac{\partial v_Z}{\partial y} - A_{55}\frac{\partial^2 w_0}{\partial x^2} \\
&- A_{44}\frac{\partial^2 w_0}{\partial y^2} - B_{55}\frac{\partial^2 w_1}{\partial x^2} - B_{44}\frac{\partial^2 w_1}{\partial y^2} - D_{55}\frac{\partial^2 w_Z}{\partial x^2} \\
&- D_{44}\frac{\partial^2 w_Z}{\partial y^2} + q_0 = I_0 \ddot{w}_0 + I_1 \ddot{w}_1 + I_2 \ddot{w}_Z
\end{aligned} \tag{46}$$

$$\begin{aligned}\delta u_1 : & -B_{11}\frac{\partial^2 u_0}{\partial x^2} - B_{66}\frac{\partial^2 u_0}{\partial y^2} - D_{11}\frac{\partial^2 u_1}{\partial x^2} + A_{55}u_1 - D_{66}\frac{\partial^2 u_1}{\partial y^2} \\ & - N_{11}\frac{\partial^2 u_Z}{\partial x^2} + H_{55}u_Z + N_{66}\frac{\partial^2 u_Z}{\partial y^2} - (B_{12}+B_{66})\frac{\partial^2 v_0}{\partial x\partial y} \\ & - (D_{12}+D_{66})\frac{\partial^2 v_1}{\partial x\partial y} - (N_{12}+N_{66})\frac{\partial^2 v_Z}{\partial x\partial y} - A_{13}\frac{\partial w_0}{\partial x} \\ & + (-B_{13}+B_{55})\frac{\partial w_1}{\partial x} + (G_{55}+O_{55}+G_{13})\frac{\partial w_Z}{\partial x} \\ & = I_1\ddot{u}_0 + I_2\ddot{u}_1 + I_7\ddot{u}_Z \end{aligned} \tag{47}$$

$$\begin{aligned}\delta v_1 : & -(B_{12}+B_{66})\frac{\partial^2 u_0}{\partial x\partial y} - (D_{12}+D_{66})\frac{\partial^2 u_1}{\partial x\partial y} \\ & - (N_{12}+N_{66})\frac{\partial^2 u_Z}{\partial x\partial y} - B_{22}\frac{\partial^2 v_0}{\partial y^2} - B_{66}\frac{\partial^2 v_0}{\partial x^2} - D_{22}\frac{\partial^2 v_1}{\partial y^2} \\ & + A_{44}v_1 - D_{66}\frac{\partial^2 v_1}{\partial x^2} - N_{22}\frac{\partial^2 v_Z}{\partial y^2} + H_{44}v_Z - N_{66}\frac{\partial^2 v_Z}{\partial x^2} \\ & - A_{23}\frac{\partial w_0}{\partial y} + (-B_{23}+B_{44})\frac{\partial w_1}{\partial y} + (G_{44}+O_{44}+G_{23})\frac{\partial w_Z}{\partial y} \\ & = I_1\ddot{v}_0 + I_2\ddot{v}_1 + I_7\ddot{v}_Z \end{aligned} \tag{48}$$

$$\begin{aligned}\delta w_1 : & -A_{55}\frac{\partial u_0}{\partial x} + (-B_{55}+B_{13})\frac{\partial u_1}{\partial x} + (-D_{55}+2D_{13})\frac{\partial u_Z}{\partial x} \\ & - A_{44}\frac{\partial v_0}{\partial y} + (-B_{44}+B_{23})\frac{\partial v_1}{\partial y} + (-D_{44}+2D_{23})\frac{\partial v_Z}{\partial y} \\ & - B_{55}\frac{\partial^2 w_0}{\partial x^2} - B_{44}\frac{\partial^2 w_0}{\partial y^2} - D_{55}\frac{\partial^2 w_1}{\partial x^2} + A_{33}w_1 - D_{44}\frac{\partial^2 w_1}{\partial y^2} \\ & - E_{55}\frac{\partial^2 w_Z}{\partial x^2} + B_{33}w_Z - E_{44}\frac{\partial^2 w_Z}{\partial y^2} = I_1\ddot{w}_0 + I_2\ddot{w}_1 + I_3\ddot{w}_Z \end{aligned} \tag{49}$$

$$\begin{aligned}\delta u_Z : & G_{11}\frac{\partial^2 u_0}{\partial x^2} + G_{66}\frac{\partial^2 u_0}{\partial y^2} - N_{11}\frac{\partial^2 u_1}{\partial x^2} + H_{55}u_1 - N_{66}\frac{\partial^2 u_1}{\partial y^2} + R_{55}u_Z \\ & + (J_{11}+J_{66})\frac{\partial^2 u_Z}{\partial x^2} + (G_{12}+G_{66})\frac{\partial^2 v_0}{\partial x\partial y} - (N_{12}+N_{66})\frac{\partial^2 v_1}{\partial x\partial y} \\ & + (J_{12}+J_{66})\frac{\partial^2 v_Z}{\partial x\partial y} - 2B_{13}\frac{\partial w_0}{\partial x} + (-2D_{13}+D_{55})\frac{\partial w_1}{\partial x} \\ & + (P_{55}-2N_{55}-2N_{13})\frac{\partial w_Z}{\partial x} = I_5\ddot{u}_0 + I_7\ddot{u}_1 + I_6\ddot{u}_Z \end{aligned} \tag{50}$$

$$\begin{aligned}\delta v_Z : & (G_{12}+G_{66})\frac{\partial^2 u_0}{\partial x\partial y} - (N_{12}+N_{66})\frac{\partial^2 u_1}{\partial x\partial y} + (J_{12}+J_{66})\frac{\partial^2 u_Z}{\partial x\partial y} \\ & + G_{22}\frac{\partial^2 v_0}{\partial y^2} + G_{66}\frac{\partial^2 v_0}{\partial x^2} - N_{22}\frac{\partial^2 v_1}{\partial y^2} + H_{44}v_1 - N_{66}\frac{\partial^2 v_1}{\partial x^2} + R_{44}v_Z \\ & + J_{22}\frac{\partial^2 v_Z}{\partial y^2} + J_{66}\frac{\partial^2 v_Z}{\partial x^2} - 2B_{23}\frac{\partial w_0}{\partial y} + (-2D_{23}+D_{44})\frac{\partial w_1}{\partial y} \\ & + (P_{44}-2N_{44}-2N_{23})\frac{\partial w_Z}{\partial y} = I_5\ddot{v}_0 + I_7\ddot{v}_1 + I_6\ddot{v}_Z \end{aligned} \tag{51}$$

$$\begin{aligned}\delta w_Z : & -H_{55}\frac{\partial u_0}{\partial x} - (G_{55}+O_{55}+G_{13})\frac{\partial u_1}{\partial x} - (P_{55}-2N_{55}-2N_{13})\frac{\partial u_Z}{\partial x} \\ & - H_{44}\frac{\partial v_0}{\partial y} - (G_{44}+O_{44}+G_{23})\frac{\partial v_1}{\partial y} - (P_{44}-2N_{44}-2N_{23})\frac{\partial v_Z}{\partial y} \\ & - D_{55}\frac{\partial^2 w_0}{\partial x^2} - D_{44}\frac{\partial^2 w_0}{\partial y^2} - E_{55}\frac{\partial^2 w_1}{\partial x^2} + 2B_{33}w_1 - E_{44}\frac{\partial^2 w_1}{\partial y^2} \\ & - F_{55}\frac{\partial^2 w_Z}{\partial x^2} + 4D_{33}w_Z - F_{44}\frac{\partial^2 w_Z}{\partial y^2} + q_2 = I_2\ddot{w}_0 + I_3\ddot{w}_1 + I_4\ddot{w}_Z \end{aligned} \tag{52}$$

Nothing N_l as the number of mathematical layers across the thickness direction, the stiffness components can be computed as follows.

$$\begin{aligned} A_{ij} &= \sum_{k=1}^{NL} c_{ij}^k (z_{k+1} - z_k) \\ B_{ij} &= \frac{1}{2}\sum_{k=1}^{NL} c_{ij}^k (z_{k+1}^2 - z_k^2) \\ D_{ij} &= \frac{1}{3}\sum_{k=1}^{NL} c_{ij}^k (z_{k+1}^3 - z_k^3) \\ E_{ij} &= \frac{1}{4}\sum_{k=1}^{NL} c_{ij}^k (z_{k+1}^4 - z_k^4) \\ F_{ij} &= \frac{1}{5}\sum_{k=1}^{NL} c_{ij}^k (z_{k+1}^5 - z_k^5) \\ G_{ij} &= \sum_{k=1}^{NL} c_{ij}^k \frac{h_k}{\pi}\left[\cos\left(\frac{\pi z_{k+1}}{h_k}\right) - \cos\left(\frac{\pi z_k}{h_k}\right)\right] \\ H_{ij} &= \sum_{k=1}^{NL} c_{ij}^k \left[\sin\left(\frac{\pi z_{k+1}}{h_k}\right) - \sin\left(\frac{\pi z_k}{h_k}\right)\right] \\ J_{ij} &= \sum_{k=1}^{NL} c_{ij}^k \left[\frac{h_k}{4\pi}\left[\sin\left(\frac{2\pi z_{k+1}}{h_k}\right) - \sin\left(\frac{2\pi z_k}{h_k}\right)\right] - \frac{1}{2}(z_{k+1} - z_k)\right] \\ N_{ij} &= \sum_{k=1}^{NL} c_{ij}^k \left[\left(\frac{h_k}{\pi}\right)^2\left(\sin\left(\frac{\pi z_{k+1}}{h_k}\right) - \sin\left(\frac{\pi z_k}{h_k}\right)\right) - \frac{h_k}{\pi}\left(z_{k+1}\cos\left(\frac{\pi z_{k+1}}{h_k}\right) - z_k\cos\left(\frac{\pi z_k}{h_k}\right)\right)\right] \\ O_{ij} &= \sum_{k=1}^{NL} c_{ij}^k \left[z_{k+1}\sin\left(\frac{\pi z_{k+1}}{h_k}\right) - z_k\sin\left(\frac{\pi z_k}{h_k}\right)\right] \\ P_{ij} &= \sum_{k=1}^{NL} c_{ij}^k \left[z_{k+1}^2\sin\left(\frac{\pi z_{k+1}}{h_k}\right) - z_k^2\sin\left(\frac{\pi z_k}{h_k}\right)\right] \\ R_{ij} &= \sum_{k=1}^{NL} c_{ij}^k \left[\frac{\pi}{4h_k}\left[\sin\left(\frac{2\pi z_{k+1}}{h_k}\right) - \sin\left(\frac{2\pi z_k}{h_k}\right)\right] + \frac{1}{2}\left(\frac{\pi}{h_k}\right)^2 (z_{k+1} - z_k)\right] \end{aligned} \tag{53}$$

and

$$\begin{aligned} I_0 &= \sum_{k=1}^{NL} \rho^k (z_{k+1} - z_k) \\ I_1 &= \frac{1}{2}\sum_{k=1}^{NL} \rho^k (z_{k+1}^2 - z_k^2) \\ I_2 &= \frac{1}{3}\sum_{k=1}^{NL} \rho^k (z_{k+1}^3 - z_k^3) \\ I_3 &= \frac{1}{4}\sum_{k=1}^{NL} \rho^k (z_{k+1}^4 - z_k^4) \\ I_4 &= \frac{1}{5}\sum_{k=1}^{NL} \rho^k (z_{k+1}^5 - z_k^5) \\ I_5 &= -\sum_{k=1}^{NL} \rho^k \frac{h_k}{\pi}\left[\cos\left(\frac{\pi z_{k+1}}{h_k}\right) - \cos\left(\frac{\pi z_k}{h_k}\right)\right] \\ I_6 &= \sum_{k=1}^{NL} \rho^k \left[\frac{1}{2}(z_{k+1} - z_k) - \frac{h_k}{4\pi}\left[\sin\left(\frac{2\pi z_{k+1}}{h_k}\right) - \sin\left(\frac{2\pi z_k}{h_k}\right)\right]\right] \\ I_7 &= \sum_{k=1}^{NL} \rho^k \left[\left(\frac{h_k}{\pi}\right)^2\left(\sin\left(\frac{\pi z_{k+1}}{h_k}\right) - \sin\left(\frac{\pi z_k}{h_k}\right)\right) - \frac{h_k}{\pi}\left(z_{k+1}\cos\left(\frac{\pi z_{k+1}}{h_k}\right) - z_k\cos\left(\frac{\pi z_k}{h_k}\right)\right)\right] \end{aligned} \tag{54}$$

where h_k is the thickness of each layer and z_k,z_{k+1} are the lower and upper z coordinate for each layer k.

2.8. Natural boundary conditions

This meshless method based on collocation with radial basis functions needs the imposition of essential (e.g. $w = 0$) and mechanical (e.g. $M_{xx} = 0$) boundary conditions. Assuming a rectangular plate (for the sake of simplicity) Eqs. (30) are expressed as follows.

Given the number of degrees of freedom, at each boundary point at edges $x = min$ or $x = max$ we impose:

$$M_{xx1} = A_{11}\frac{\partial u_0}{\partial x} + B_{11}\frac{\partial u_1}{\partial x} - G_{11}\frac{\partial u_Z}{\partial x} + A_{12}\frac{\partial v_0}{\partial y} + B_{12}\frac{\partial v_1}{\partial y} - G_{12}\frac{\partial v_Z}{\partial y} \tag{55}$$

$$M_{xx2} = B_{11}\frac{\partial u_0}{\partial x} + D_{11}\frac{\partial u_1}{\partial x} + N_{11}\frac{\partial u_Z}{\partial x} + B_{12}\frac{\partial v_0}{\partial y} + D_{12}\frac{\partial v_1}{\partial y} + N_{12}\frac{\partial v_Z}{\partial y} + A_{13}w_0 + B_{13}w_1 - G_{13}w_Z \tag{56}$$

$$M_{xx3} = -G_{11}\frac{\partial u_0}{\partial x} + N_{11}\frac{\partial u_1}{\partial x} - J_{11}\frac{\partial u_Z}{\partial x} - G_{12}\frac{\partial v_0}{\partial y} + N_{12}\frac{\partial v_1}{\partial y} - J_{12}\frac{\partial v_Z}{\partial y} + 2B_{13}w_0 + 2D_{13}w_1 + 2N_{13}w_Z \tag{57}$$

$$M_{xx4} = A_{66}\frac{\partial u_0}{\partial y} + B_{66}\frac{\partial u_1}{\partial y} - G_{66}\frac{\partial u_Z}{\partial y} + A_{66}\frac{\partial v_0}{\partial x} + B_{66}\frac{\partial v_1}{\partial x} - G_{66}\frac{\partial v_Z}{\partial x} \tag{58}$$

$$M_{xx5} = B_{66}\frac{\partial u_0}{\partial y} + D_{66}\frac{\partial u_1}{\partial y} + N_{66}\frac{\partial u_Z}{\partial y} + B_{66}\frac{\partial v_0}{\partial x} + D_{66}\frac{\partial v_1}{\partial x} + N_{66}\frac{\partial v_Z}{\partial x} \tag{59}$$

$$M_{xx6} = -G_{66}\frac{\partial u_0}{\partial y} + N_{66}\frac{\partial u_1}{\partial y} - J_{66}\frac{\partial u_Z}{\partial y} - G_{66}\frac{\partial v_0}{\partial x} + N_{66}\frac{\partial v_1}{\partial x} - J_{66}\frac{\partial v_Z}{\partial x} \tag{60}$$

$$M_{xx7} = A_{55}\frac{\partial w_0}{\partial x} + B_{55}\frac{\partial w_1}{\partial x} + D_{55}\frac{\partial w_Z}{\partial x} \tag{61}$$

$$M_{xx8} = A_{55}u_0 + B_{55}u_1 + D_{55}u_Z + B_{55}\frac{\partial w_0}{\partial x} + D_{55}\frac{\partial w_1}{\partial x} + E_{55}\frac{\partial w_Z}{\partial x} \tag{62}$$

$$M_{xx9} = H_{55}u_0 + (G_{55} + O_{55})u_1 + (P_{55} - 2N_{55})u_Z + D_{55}\frac{\partial w_0}{\partial x} + E_{55}\frac{\partial w_1}{\partial x} + F_{55}\frac{\partial w_Z}{\partial x} \tag{63}$$

Similarly, given the number of degrees of freedom, at each boundary point at edges $y = min$ or $y = max$ we impose:

$$M_{yy1} = A_{66}\frac{\partial u_0}{\partial y} + B_{66}\frac{\partial u_1}{\partial y} - G_{66}\frac{\partial u_Z}{\partial y} + A_{66}\frac{\partial v_0}{\partial x} + B_{66}\frac{\partial v_1}{\partial x} - G_{66}\frac{\partial v_Z}{\partial x} \tag{64}$$

$$M_{yy2} = B_{66}\frac{\partial u_0}{\partial y} + D_{66}\frac{\partial u_1}{\partial y} + N_{66}\frac{\partial u_Z}{\partial y} + B_{66}\frac{\partial v_0}{\partial x} + D_{66}\frac{\partial v_1}{\partial x} + N_{66}\frac{\partial v_Z}{\partial x} \tag{65}$$

$$M_{yy3} = -G_{66}\frac{\partial u_0}{\partial y} + N_{66}\frac{\partial u_1}{\partial y} - J_{66}\frac{\partial u_Z}{\partial y} - G_{66}\frac{\partial v_0}{\partial x} + N_{66}\frac{\partial v_1}{\partial x} - J_{66}\frac{\partial v_Z}{\partial x} \tag{66}$$

$$M_{yy4} = A_{12}\frac{\partial u_0}{\partial x} + B_{12}\frac{\partial u_1}{\partial x} - G_{12}\frac{\partial u_Z}{\partial x} + A_{22}\frac{\partial v_0}{\partial y} + B_{22}\frac{\partial v_1}{\partial y} - G_{22}\frac{\partial v_Z}{\partial y} \tag{67}$$

$$M_{yy5} = B_{12}\frac{\partial u_0}{\partial x} + D_{12}\frac{\partial u_1}{\partial x} + N_{12}\frac{\partial u_Z}{\partial x} + B_{22}\frac{\partial v_0}{\partial y} + D_{22}\frac{\partial v_1}{\partial y} + N_{22}\frac{\partial v_Z}{\partial y} \tag{68}$$

$$M_{yy6} = -G_{12}\frac{\partial u_0}{\partial x} + N_{12}\frac{\partial u_1}{\partial x} - J_{12}\frac{\partial u_Z}{\partial x} - G_{22}\frac{\partial v_0}{\partial y} + N_{22}\frac{\partial v_1}{\partial y} - J_{22}\frac{\partial v_Z}{\partial y} \tag{69}$$

$$M_{yy7} = A_{44}\frac{\partial w_0}{\partial y} + B_{44}\frac{\partial w_1}{\partial y} + D_{44}\frac{\partial w_Z}{\partial y} \tag{70}$$

$$M_{yy8} = A_{44}v_0 + B_{44}v_1 + D_{44}v_Z + B_{44}\frac{\partial w_0}{\partial y} + D_{44}\frac{\partial w_1}{\partial y} + E_{44}\frac{\partial w_Z}{\partial y} \tag{71}$$

$$M_{yy9} = H_{44}v_0 + (G_{44} + O_{44})v_1 + (P_{44} - 2N_{44})v_Z + D_{44}\frac{\partial w_0}{\partial y} + E_{44}\frac{\partial w_1}{\partial y} + F_{44}\frac{\partial w_Z}{\partial y} \tag{72}$$

with A_{ij}, B_{ij}, D_{ij}, E_{ij}, F_{ij}, G_{ij}, H_{ij}, J_{ij}, N_{ij}, O_{ij}, P_{ij}, R_{ij} already given in (53).

3. The radial basis function method

For the sake of completeness we present here the basics of collocation with radial basis functions for static and vibrations problems.

3.1. The static problem

In this section the formulation of a global unsymmetrical collocation RBF-based method to compute elliptic operators is presented. Consider a linear elliptic partial differential operator L and a bounded region Ω in $\mathbb{R}^n$ with some boundary $\partial\Omega$. In the static problems we seek the computation of displacements (u) from the global system of equations

$$\mathcal{L}\mathbf{u} = \mathbf{f} \text{ in } \Omega; \quad \mathcal{L}_B\mathbf{u} = \mathbf{g} \text{ on } \partial\Omega \tag{73}$$

where $\mathcal{L}, \mathcal{L}_B$ are linear operators in the domain and on the boundary, respectively. The right-hand sides in (73) represent the external forces applied on the plate and the boundary conditions applied along the perimeter of the plate, respectively. The PDE problem defined in (73) will be replaced by a finite problem, defined by an algebraic system of equations, after the radial basis expansions.

3.2. The eigenproblem

The eigenproblem looks for eigenvalues (λ) and eigenvectors ($\mathbf{u}$) that satisfy

$$\mathcal{L}\mathbf{u} + \lambda\mathbf{u} = 0 \text{ in } \Omega; \quad \mathcal{L}_B\mathbf{u} = 0 \text{ on } \partial\Omega \tag{74}$$

As in the static problem, the eigenproblem defined in (74) is replaced by a finite-dimensional eigenvalue problem, based on RBF approximations.

3.3. Radial basis functions approximations

The radial basis function (ϕ) approximation of a function (u) is given by

$$\tilde{\mathbf{u}}(\mathbf{x}) = \sum_{i=1}^{N} \alpha_i \phi(\|x - y_i\|_2), \quad \mathbf{x} \in \mathbb{R}^n \tag{75}$$

where y_i, $i = 1, \ldots, N$ is a finite set of distinct points (centers) in $\mathbb{R}^n$. Although we can use many RBFs, in this paper we restrict to the Wendland function, defined as

$$\phi(r) = (1 - c\ r)_+^8 (32(c\ r)^3 + 25(c\ r)^2 + 8c\ r + 1) \tag{76}$$

where the Euclidian distance r is real and non-negative and c is a positive shape parameter. The shape parameter (c) was obtained by an optimization procedure, as detailed in Ferreira and Fasshauer [26].

Considering N distinct interpolations, and knowing $u(x_j)$, $j = 1, 2, \ldots, N$, we find α_i by the solution of a $N \times N$ linear system

$$\mathbf{A}\boldsymbol{\alpha} = \mathbf{u} \tag{77}$$

where $\mathbf{A} = [\phi(\|x - y_i\|_2)]_{N\times N}$, $\boldsymbol{\alpha} = [\alpha_1, \alpha_2, \ldots, \alpha_N]^T$ and $\mathbf{u} = [u(x_1), u(x_2), \ldots, u(x_N)]^T$.

3.4. Solution of the static problem

The solution of a static problem by radial basis functions considers N_I nodes in the domain and N_B nodes on the boundary, with a total number of nodes $N = N_I + N_B$. We denote the sampling points by $x_i \in \Omega$, $i = 1, \ldots, N_I$ and $x_i \in \partial\Omega$, $i = N_I + 1, \ldots, N$. At the points in the domain we solve the following system of equations

$$\sum_{i=1}^{N} \alpha_i \mathcal{L}\phi(\|x - y_i\|_2) = \mathbf{f}(x_j), \quad j = 1, 2, \ldots, N_I \tag{78}$$

or

$$\mathcal{L}^I \boldsymbol{\alpha} = \mathbf{F} \tag{79}$$

where

$$\mathcal{L}^I = [\mathcal{L}\phi(\|x - y_i\|_2)]_{N_I\times N} \tag{80}$$

At the points on the boundary, we impose boundary conditions as

$$\sum_{i=1}^{N} \alpha_i \mathcal{L}_B\phi(\|x - y_i\|_2) = \mathbf{g}(x_j), \quad j = N_I + 1, \ldots, N \tag{81}$$

or

$$\mathbf{B}\boldsymbol{\alpha} = \mathbf{G} \tag{82}$$

where

$$\mathbf{B} = \mathcal{L}_B\phi[(\|x_{N_I+1} - y_j\|_2)]_{N_B\times N}$$

Therefore, we can write a finite-dimensional static problem as

$$\begin{bmatrix} \mathcal{L}^I \\ \mathbf{B} \end{bmatrix} \boldsymbol{\alpha} = \begin{bmatrix} \mathbf{F} \\ \mathbf{G} \end{bmatrix} \tag{83}$$

By inverting the system (83), we obtain the vector $\boldsymbol{\alpha}$. We then obtain the solution $\mathbf{u}$ using the interpolation Eq. (75).

3.5. Solution of the eigenproblem

We consider N_I nodes in the interior of the domain and N_B nodes on the boundary, with $N = N_I + N_B$. We denote interpolation points by $x_i \in \Omega$, $i = 1, \ldots, N_I$ and $x_i \in \partial\Omega$, $i = N_I + 1, \ldots, N$. At the points in the domain, we define the eigenproblem as

$$\sum_{i=1}^{N} \alpha_i \mathcal{L}\phi(\|x - y_i\|_2) = \lambda\tilde{\mathbf{u}}(x_j), \quad j = 1, 2, \ldots, N_I \tag{84}$$

or

$$\mathcal{L}^I \boldsymbol{\alpha} = \lambda\tilde{\mathbf{u}}^I \tag{85}$$

where

$$\mathcal{L}^I = [\mathcal{L}\phi(\|x - y_i\|_2)]_{N_I\times N} \tag{86}$$

At the points on the boundary, we enforce the boundary conditions as

$$\sum_{i=1}^{N} \alpha_i \mathcal{L}_B\phi(\|x - y_i\|_2) = 0, \quad j = N_I + 1, \ldots, N \tag{87}$$

or

$$\mathbf{B}\boldsymbol{\alpha} = 0 \tag{88}$$

Eqs. (85) and (88) can now be solved as a generalized eigenvalue problem

$$\begin{bmatrix} \mathcal{L}^I \\ \mathbf{B} \end{bmatrix} \boldsymbol{\alpha} = \lambda \begin{bmatrix} \mathbf{A}^I \\ \mathbf{0} \end{bmatrix} \boldsymbol{\alpha} \tag{89}$$

where

$$\mathbf{A}^I = \phi[(\|x_{N_I} - y_j\|_2)]_{N_I\times N}$$

3.6. Discretization of the equations of motion and boundary conditions

The radial basis collocation method follows a simple implementation procedure. Taking Eq. (83), we compute

$$\boldsymbol{\alpha} = \begin{bmatrix} L^I \\ \mathbf{B} \end{bmatrix}^{-1} \begin{bmatrix} \mathbf{F} \\ \mathbf{G} \end{bmatrix} \tag{90}$$

This $\boldsymbol{\alpha}$ vector is then used to obtain solution $\tilde{\mathbf{u}}$, by using (75). If derivatives of $\tilde{\mathbf{u}}$ are needed, such derivatives are computed as

$$\frac{\partial\tilde{\mathbf{u}}}{\partial x} = \sum_{j=1}^{N} \alpha_j \frac{\partial\phi_j}{\partial x}; \quad \frac{\partial^2\tilde{\mathbf{u}}}{\partial x^2} = \sum_{j=1}^{N} \alpha_j \frac{\partial^2\phi_j}{\partial x^2}, \quad \text{etc.} \tag{91}$$

In the present collocation approach, we need to impose essential and natural boundary conditions. Consider, for example, the condition $w_0 = 0$, on a simply supported or clamped edge. We enforce the conditions by interpolating as

$$w_0 = 0 \rightarrow \sum_{j=1}^{N} \alpha_j^{W_0} \phi_j = 0 \tag{92}$$

Other boundary conditions are interpolated in a similar way.

3.7. Free vibrations problems

For free vibration problems we set the external force to zero, and assume harmonic solution in terms of displacements u_0, u_1, u_Z, v_0, v_1, v_Z, w_0, w_1, w_Z as

$$\begin{aligned} &u_0 = U_0(w,y)e^{i\omega t}; \quad u_1 = U_1(w,y)e^{i\omega t}; \quad u_Z = U_Z(w,y)e^{i\omega t};\\ &v_0 = V_0(w,y)e^{i\omega t}; \quad v_1 = V_1(w,y)e^{i\omega t}; \quad v_Z = V_Z(w,y)e^{i\omega t};\\ &w_0 = W_0(w,y)e^{i\omega t}; \quad w_1 = W_1(w,y)e^{i\omega t}; \quad w_Z = W_Z(w,y)e^{i\omega t} \end{aligned} \tag{93}$$

where ω is the frequency of natural vibration. Substituting the harmonic expansion into Eqs. (89) in terms of the amplitudes U_0, U_1, U_Z, V_0, V_1, V_Z, W_0, W_1, W_Z, we may obtain the natural frequencies and vibration modes for the plate problem, by solving the eigenproblem

$$[\mathcal{L} - \omega^2\mathcal{G}]\mathbf{X} = \mathbf{0} \tag{94}$$

where $\mathcal{L}$ collects all stiffness terms and $\mathcal{G}$ collects all terms related to the inertial terms. In (94) $\mathbf{X}$ are the modes of vibration associated with the natural frequencies defined as ω.

Table 1
FGM isotropic plate with polynomial material law [2]. Effect of transverse normal strain ϵ_{zz} for a bending problem.

p		ϵ_{zz}	$\bar{\sigma}_{xx}(h/3)$			$\bar{u}_z(0,0)$		
			$a/h = 4$	$a/h = 10$	$a/h = 100$	$a/h = 4$	$a/h = 10$	$a/h = 100$
1	Ref. [27]	≠0	0.6221	1.5064	14.969	0.7171	0.5875	0.5625
	CLT	0	0.8060	2.0150	20.150	0.5623	0.5623	0.5623
	FSDT ($k = 5/6$)	0	0.8060	2.0150	20.150	0.7291	0.5889	0.5625
	GSDT [2]	0		1.4894			0.5889	
	Ref. [9] $N = 4$	0	0.7856	2.0068	20.149	0.7289	0.5890	0.5625
	Ref. [9] $N = 4$	≠0	0.6221	1.5064	14.969	0.7171	0.5875	0.5625
	Present 13^2 grid	≠0	0.5925	1.4939	14.901	0.6997	0.5844	0.5596
	Present 17^2 grid	≠0	0.5925	1.4945	14.957	0.6998	0.5845	0.5622
	Present 21^2 grid	≠0	0.5925	1.4945	14.969	0.6997	0.5845	0.5624
4	Ref. [27]	≠0	0.4877	1.1971	11.923	1.1585	0.8821	0.8286
	CLT	0	0.6420	1.6049	16.049	0.8281	0.8281	0.8281
	FSDT ($k = 5/6$)	0	0.6420	1.6049	16.049	1.1125	0.8736	0.828
	GSDT [2]	0		1.1783			0.8651	
	Ref. [9] $N = 4$	0	0.5986	1.5874	16.047	1.1673	0.8828	0.8286
	Ref. [9] $N = 4$	≠0	0.4877	1.1971	11.923	1.1585	0.8821	0.8286
	Present 13^2 grid	≠0	0.4404	1.1780	11.894	1.1178	0.8749	0.8251
	Present 17^2 grid	≠0	0.4404	1.1783	11.923	1.1178	0.8750	0.8284
	Present 21^2 grid	≠0	0.4404	1.1783	11.932	1.1178	0.8750	0.8286
10	Ref. [27]	≠0	0.3695	0.8965	8.9077	1.3745	1.0072	0.9361
	CLT	0	0.4796	1.1990	11.990	0.9354	0.9354	0.9354
	FSDT ($k = 5/6$)	0	0.4796	1.1990	11.990	1.3178	0.9966	0.9360
	GSDT [2]	0		0.8775			1.0089	
	Ref. [9] $N = 4$	0	0.4345	1.1807	11.989	1.3925	1.0090	0.9361
	Ref. [9] $N = 4$	≠0	0.1478	0.8965	8.9077	1.3745	1.0072	0.9361
	Present 13^2 grid	≠0	0.3227	1.1780	11.894	1.3490	0.8749	0.8251
	Present 17^2 grid	≠0	0.3227	1.1783	11.923	1.3490	0.8750	0.8284
	Present 21^2 grid	≠0	0.3227	1.1783	11.932	1.3490	0.8750	0.8286

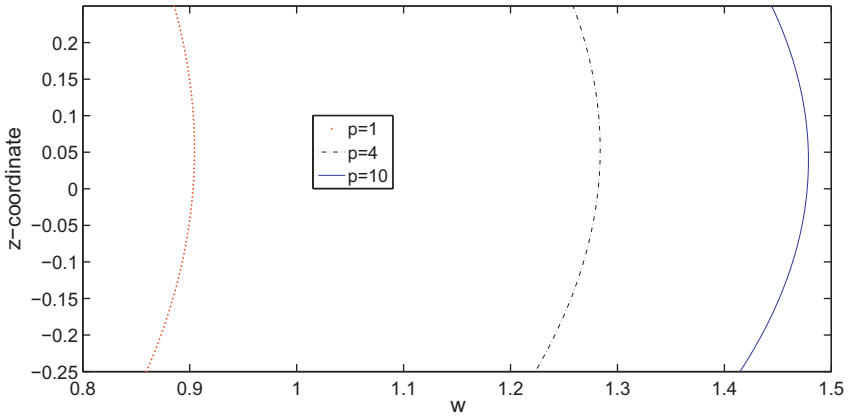

Fig. 1. FGM square plate subjected to sinusoidal load at the top, with $a/h = 4$. Displacement through the thickness direction for different values of p at the center of the plate $(\frac{a}{2}, \frac{b}{2})$.

4. Numerical examples

4.1. Bending problems

In the next examples we use the sinusoidal plate theory to analyse simply supported square (side lengths $a = b$) plates subjected to a bi-sinusoidal transverse mechanical load, of amplitude load $p_z = \bar{p}_z sin(\frac{\pi x}{a}) sin(\frac{\pi y}{b})$ applied at the top plate surface, $z = h/2$, $\bar{p}_z = 1$. Three side-to-thickness ratios (a/h) are considered 4, 10 and 100.

We consider 91 mathematical layers, in order to model the continuous variation of properties across the thickness direction.[1] We consider a Wendland C6 radial function as in (76), and a Chebyshev grid (see [26] for details).

4.1.1. Isotropic functionally graded plate

In this example, an isotropic FGM square plate with a polynomial material law, as given by Zenkour [2] is considered. The plate is graded from aluminum (bottom surface) to alumina (top surface) materials. The following functional relationship is considered for modulus of elasticity $E(z)$ in the thickness direction (z) [2]:

$$E(z) = E_m + (E_c - E_m)\left(\frac{2z+h}{2h}\right)^p \tag{95}$$

where $E_m = 70$ GPa and $E_c = 380$ GPa are the corresponding modulus of elasticity of the metal and ceramic phases, respectively; p is the (positive number) volume fraction exponent. The Poisson's ratio is considered constant ($\nu = 0.3$).

[1] A significant number of mathematical layers is needed to ensure correct material properties at each thickness position.

The in-plane displacements, the transverse displacements, the normal stresses and the in-plane and transverse shear stresses are respectively presented in normalized form as

$$\bar{u}_z = \frac{10h^3 E_c}{a^4 \bar{p}_z} u_z, \quad \bar{\sigma}_{xx} = \frac{h}{a\bar{p}_z}\sigma_{xx}, \quad \bar{\sigma}_{xz} = \frac{h}{a\bar{p}_z}\sigma_{xz}, \quad \bar{\sigma}_{zz} = \sigma_{zz} \tag{96}$$

The present approach with $\epsilon_{zz} \neq 0$ is compared with analytical solutions by Carrera et al. [27], the classical plate theory (CLT), the first-order shear deformation theory (FSDT), a generalized shear deformation theory by Zenkour [2] (who considered $\epsilon_{zz} = 0$), and finite element solutions by Carrera et al. [9]. We consider Chebyschev grids with 13^2,17^2 and 21^2 points. Three FGM configurations are considered by using different p exponents ($p = 1, 4, 10$). Thick ($a/h = 4$) down to thin ($a/h = 100$) plates are analysed. Normalized transverse displacements ($\bar{u}_z$) and normal stresses ($\bar{\sigma}_{xx}$) at selected points are shown in Table 1. Our approach presents very close re-

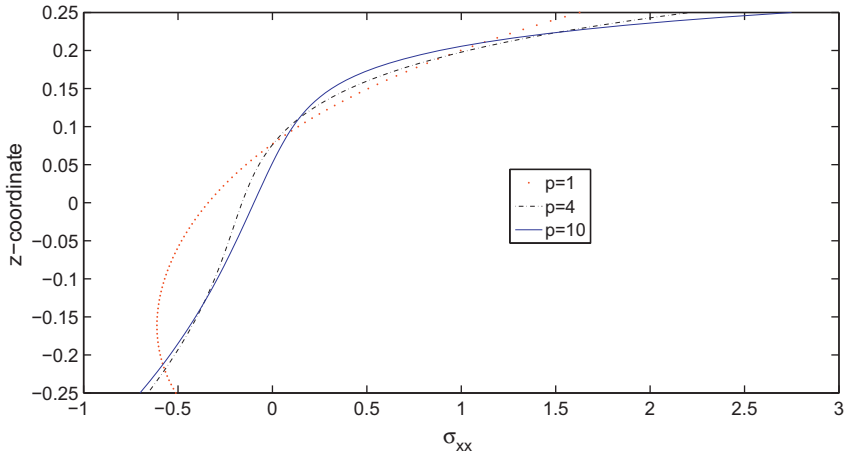

Fig. 2. FGM square plate subjected to sinusoidal load at the top, with $a/h = 4$. σ_{xx} through the thickness direction for different values of p at the center of the plate $(\frac{a}{2}, \frac{b}{2})$.

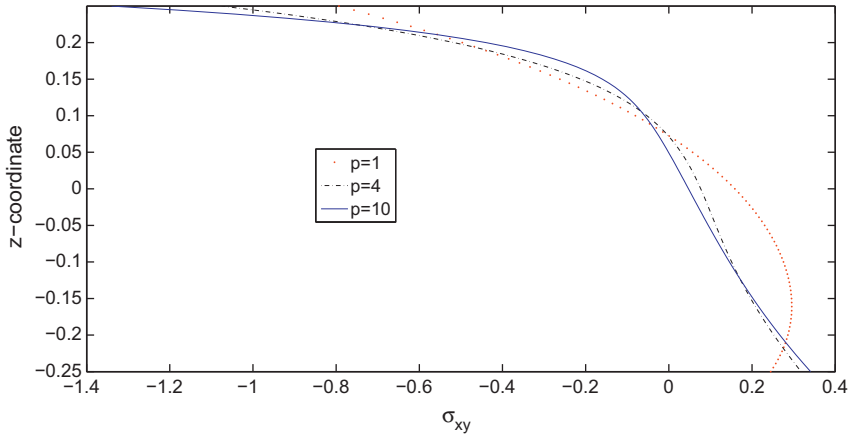

Fig. 3. FGM square plate subjected to sinusoidal load at the top, with $a/h = 4$. σ_{xy} through the thickness direction at the corner of the plate (0,0) for different values of p.

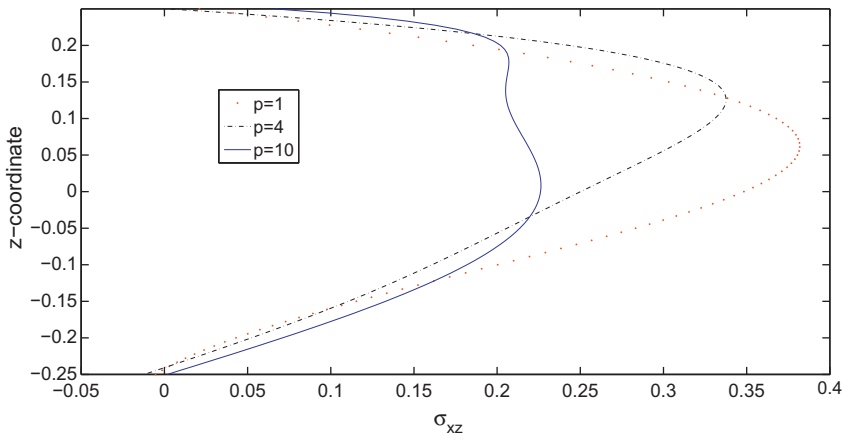

Fig. 4. FGM square plate subjected to sinusoidal load at the top, with $a/h = 4$. σ_{xz} through the thickness direction at the center of the plate $(0, \frac{b}{2})$ for different values of p.

sults to those theories that consider thickness stretching, and clearly deviates from those theories that neglect ϵ_{zz}, in particular for thicker plates. The present approach presents very close results to Carrera's analytical solution [27].

In Figs. 1–6 we present the evolution of the displacement and stresses across the thickness direction for various values of the exponent p, using a 21^2 grid. As can be seen in Fig. 6, the transverse normal component σ_{zz} cannot be neglected for the present problem.

4.1.2. Sandwich square plate with FGM core

In this example we consider a sandwich plate with total thickness h, by using a polynomial material law for the core, as given by Zenkour [2]. The bottom skin is aluminium ($E_m = 70$ GPa) with thickness $h_b = 0.1h$ and the top skin is alumina ($E_c = 380$ GPa) with thickness $h_t = 0.1h$. The core is a FGM with the following functional relationship for modulus of elasticity $E(z)$ in the thickness direction z [2]:

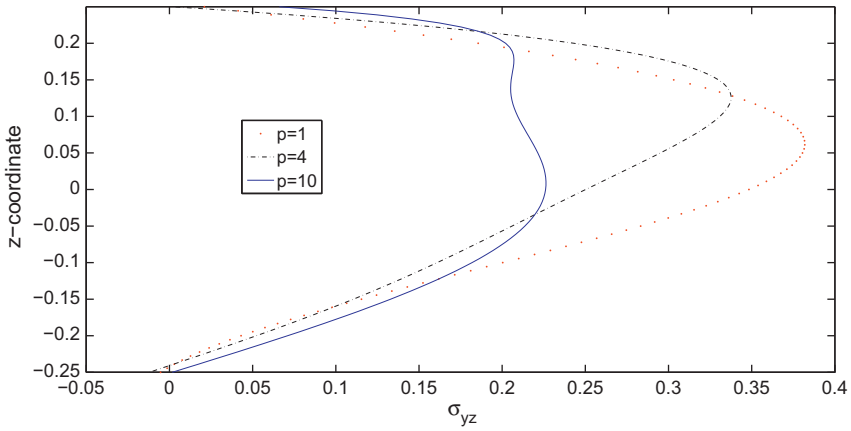

Fig. 5. FGM square plate subjected to sinusoidal load at the top, with $a/h = 4$. σ_{yz} through the thickness direction at the point $(\frac{a}{2}, 0)$ for different values of p.

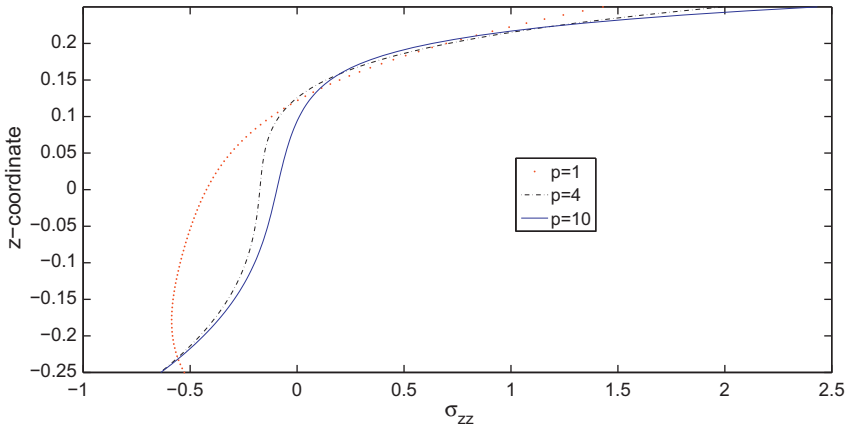

Fig. 6. FGM square plate subjected to sinusoidal load at the top, with $a/h = 4$. σ_{zz} through the thickness direction for different values of p at the center of the plate $(\frac{a}{2}, \frac{b}{2})$.

Table 2
Sandwich simply supported square plate with FGM core with polynomial material law [2] using a 19^2 grid. Effect of transverse normal strain ϵ_{zz} on σ_{xz} and transverse displacement for a bending problem.

p		ϵ_{zz}	$\bar{\sigma}_{xz}(0, \frac{b}{2}, \frac{h}{3})$			$\bar{w}(0,0,0)$		
			$a/h = 4$	$a/h = 10$	$a/h = 100$	$a/h = 4$	$a/h = 10$	$a/h = 100$
1	Ref. [9] $N = 4$	0	0.2604	0.2594	0.2593	0.7628	0.6324	0.6072
	Ref. [9] $N = 4$	$\neq 0$	0.2596	0.2593	0.2593	0.7735	0.6337	0.6072
	Present	0	0.2703	0.2718	0.2720	0.7744	0.6356	0.6092
	Present	$\neq 0$	0.2742	0.2788	0.2793	0.7416	0.6305	0.6092
4	Ref. [9] $N = 4$	0	0.2400	0.2398	0.2398	1.0930	0.8307	0.7797
	Ref. [9] $N = 4$	$\neq 0$	0.2400	0.2398	0.2398	1.0977	0.8308	0.7797
	Present	0	0.2699	0.2726	0.2728	1.0847	0.8276	0.7785
	Present	$\neq 0$	0.2723	0.2778	0.2785	1.0391	0.8202	0.7784
10	Ref. [9] $N = 4$	0	0.1932	0.1944	0.1946	1.2172	0.8740	0.8077
	Ref. [9] $N = 4$	$\neq 0$	0.1935	0.1944	0.1946	1.2240	0.8743	0.8077
	Present	0	0.1998	0.2021	0.2022	1.2212	0.8718	0.8050
	Present	$\neq 0$	0.2016	0.2059	0.2064	1.1780	0.8650	0.8050

$$E(z) = E_m + (E_c - E_m)\left(\frac{2z+h}{2h}\right)^p \tag{97}$$

where p is the (positive number) volume fraction exponent. The Poisson's ratio is considered constant $\nu = 0.3$.

The transverse displacement and the normal stresses are computed in normalized form as

$$\bar{u}_z = \frac{10h^3 E_c}{a^4 \bar{p}_z} u_z\left(\frac{a}{2}, \frac{b}{2}\right) \quad \bar{\sigma}_{xx} = \frac{h}{a\bar{p}_z}\sigma_{xx}\left(\frac{a}{2}, \frac{b}{2}\right)$$
$$\bar{\sigma}_{yy} = \frac{h}{a\bar{p}_z}\sigma_{yy}\left(\frac{a}{2}, \frac{b}{2}\right) \quad \bar{\sigma}_{zz} = \sigma_{zz}\left(\frac{a}{2}, \frac{b}{2}\right) \tag{98}$$

The shear stresses are normalized according to

Table 3
Sandwich simply supported square plate with FGM core with polynomial material law [2] using a 19^2 grid. Effect of transverse normal strain ϵ_{zz} on σ_{xy} and σ_{zz} for a bending problem. $\bar{\sigma}_{zz} = \sigma_{zz}\frac{h}{a\bar{p}_z}$.

p		ϵ_{zz}	$\bar{\sigma}_{xy}(0,0,\frac{h}{3})$		$\bar{\sigma}_{zz}(\frac{a}{2},\frac{b}{2},0)$	
			$a/h = 4$	$a/h = 100$	$a/h = 4$	$a/h = 100$
1	Ref. LD4 [28]	0	0.3007	8.4968	0.0922	0.0038
	Ref. LM4 [28]	≠0	0.3007	8.4968	0.0922	0.0038
	Present	0	0.3303	8.4882	0.1276	3.1987
	Present	≠0	0.3167	8.4911	0.0827	0.0034
5	Ref. LD4 [28]	0	0.1999	6.4942	0.0911	0.0037
	Ref. LM4 [28]	≠0	0.1996	6.4942	0.0924	0.0037
	Present	0	0.2317	6.4454	0.0777	1.9535
	Present	≠0	0.2248	6.4441	0.0522	0.0022
10	Ref. LD4 [28]	0	0.1412	5.1402	0.1064	0.0043
	Ref. LM4 [28]	≠0	0.1403	5.1401	0.1067	0.0042
	Present	0	0.1745	5.0745	0.0685	1.6978
	Present	≠0	0.1687	5.0754	0.0443	0.0018

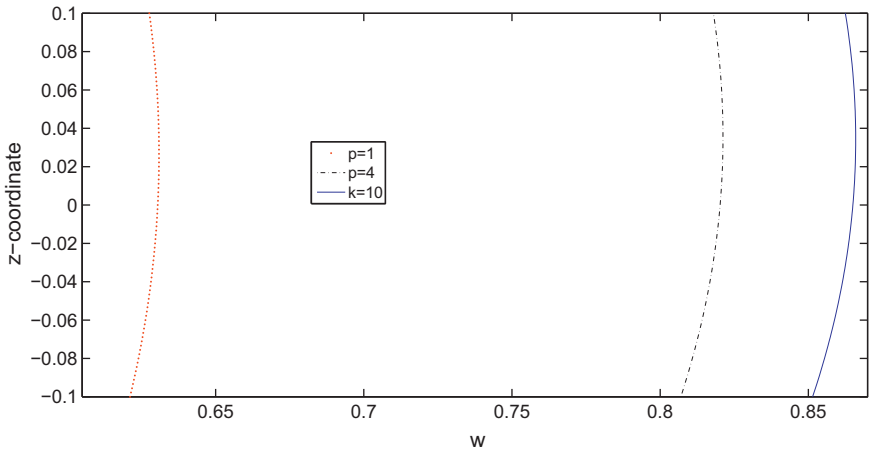

Fig. 7. Sandwich square plate with FGM core subjected to sinusoidal load at the top, with $a/h = 10$. Displacement through the thickness direction at the center of the plate $(\frac{a}{2}, \frac{b}{2})$ for different values of p.

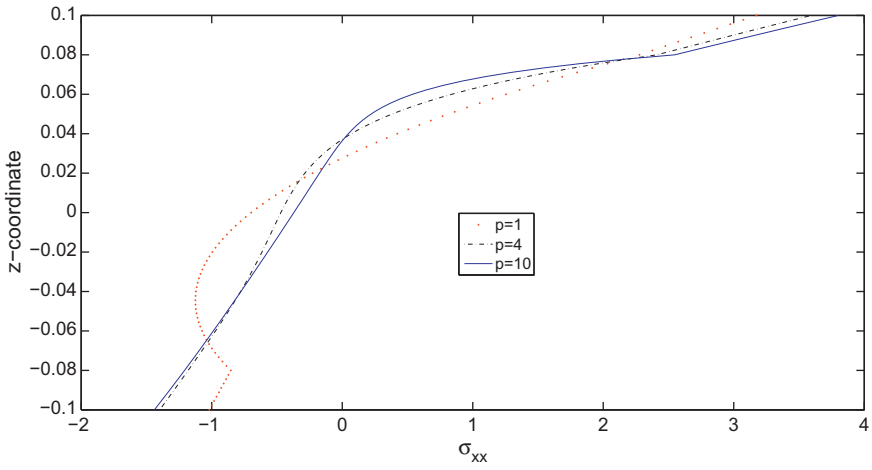

Fig. 8. Sandwich square plate with FGM core subjected to sinusoidal load at the top, with $a/h = 10$. σ_{xx} through the thickness direction at the center of the plate $(\frac{a}{2}, \frac{b}{2})$ for different values of p.

$$\bar{\sigma}_{xy} = \frac{h}{a\bar{p}_z}\sigma_{xy}(0,0); \quad \bar{\sigma}_{xz} = \frac{h}{a\bar{p}_z}\sigma_{xz}\left(0,\frac{b}{2}\right);$$
$$\bar{\sigma}_{yz} = \frac{h}{a\bar{p}_z}\sigma_{yz}\left(\frac{a}{2},0\right) \tag{99}$$

In Table 2 we present the normalized transverse displacement ($\bar{w}$) and the normalized transverse shear stress ($\bar{\sigma}_{xz}$) at selected locations. In Table 3 we present the normalized in-plane shear stress ($\bar{\sigma}_{xy}$) and the normalized transverse normal stress ($\bar{\sigma}_{zz}$) at selected

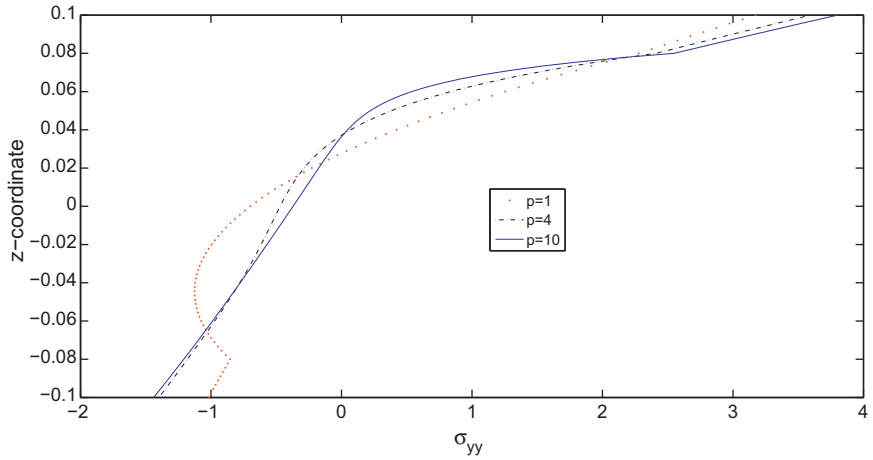

Fig. 9. Sandwich square plate with FGM core subjected to sinusoidal load at the top, with $a/h = 10$. σ_{yy} through the thickness direction at the center of the plate $(\frac{a}{2},\frac{b}{2})$ for different values of p.

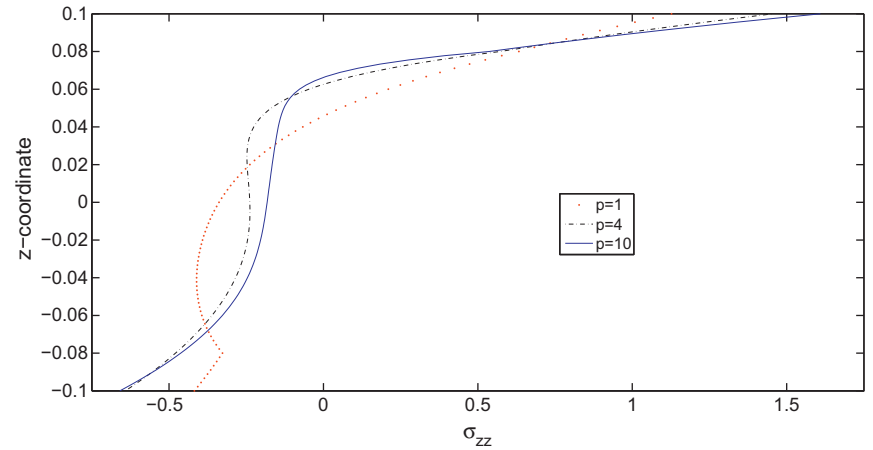

Fig. 10. Sandwich square plate with FGM core subjected to sinusoidal load at the top, with $a/h = 10$. σ_{zz} through the thickness direction at the center of the plate $(\frac{a}{2},\frac{b}{2})$ for different values of p.

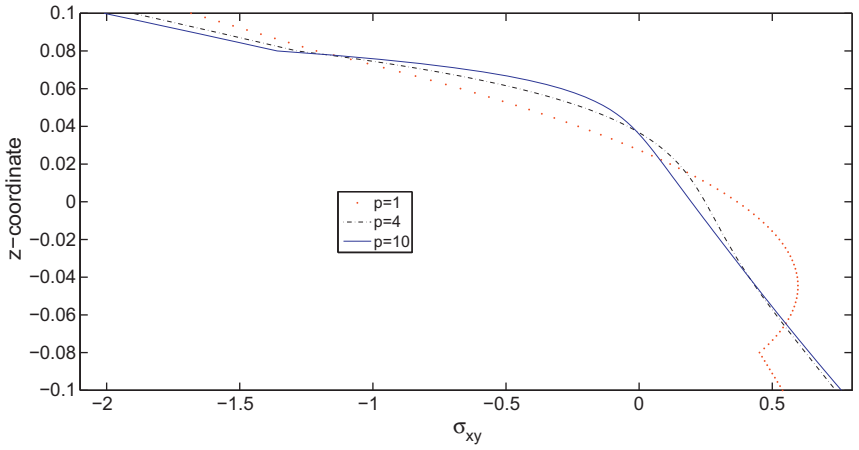

Fig. 11. Sandwich square plate with FGM core subjected to sinusoidal load at the top, with $a/h = 10$. σ_{xy} through the thickness direction at the point $(0,0)$ for different values of p.

locations. In both tables we consider three a/h ratios (4, 10 and 100), and three power-law exponents ($p = 1$, 4 and 10). We use a 19^2 Chebyshev grid and consider both $\epsilon_{zz} = 0$ and $\epsilon_{zz} \neq 0$ approaches. Our meshless results are compared in Table 2 with finite element results by Carrera et al. [9], and compare quite well for all cases. In Table 3 we compare the present approach with FEM results by Brischetto [28] and again the comparison is quite good.

n Figs. 7–13 we present the evolution of the displacement and stresses across the thickness direction for various values of the exponent p of a plate with side to thickness ratio $a/h = 10$, using a 19^2 grid.

The present numerical method presents very close results to those of Carrera et al. [9] for a $N = 4$ expansion.

The consideration of a non-zero ϵ_{zz} strain produces a significant change in the transverse displacement as well as in the normal stress. This becomes evident when we compare the present approch with that of Zenkour [2] who neglected the ϵ_{zz} strain in the formulation.

4.2. Free vibration problems

In this example, we study the free vibration behavior of simply-supported isotropic FGM plates. We consider both the $\epsilon_{zz} = 0$ and the $\epsilon_{zz} \neq 0$ cases. We compare results with an exact (analytical) solution by Vel and Batra [29], and another meshless technique by Qian et al. [8]. In order to compare results, we use the Mori–Tanaka scheme for obtaing equivalent material properties.

In Table 4 we consider thin and thick plates, with $p = 1$, and using 13^2 Chebishev points. The ϵ_{zz} effect is significant. In fact, the exact solution by Vel and Batra [29] is achieved for all cases, by allowing $\epsilon_{zz} \neq 0$. In Table 5 we compare with the same sources, varying the p exponent, for $a/h = 5$ and using 13^2 points. Our present formulation with $\epsilon_{zz} \neq 0$ matches the exact solution.

In Fig. 14 the first four frequencies are presented for $p = 1$ and using 17^2 points. In Table 6 we present the first ten frequencies for the same exponent p and compare results with those from [8] for different side-to-thickness ratios and different number of Chebishev points.

Table 4
Fundamental frequency $\bar{\omega} = \omega h\sqrt{\rho_m/E_m}$ of a SSSS isotropic functionally graded plate (Al/ZrO_2), $p = 1$, using 13^2 points.

Source	a/h		
	20	10	5
Ref. [8]	0.0149	0.0584	0.2152
Exact [29]	0.0153	0.0596	0.2192
Present, Sinus ($\epsilon_{zz} = 0$)	0.0153	0.0595	0.2184
Present, Sinus ($\epsilon_{zz} \neq 0$)	0.0153	0.0596	0.2193

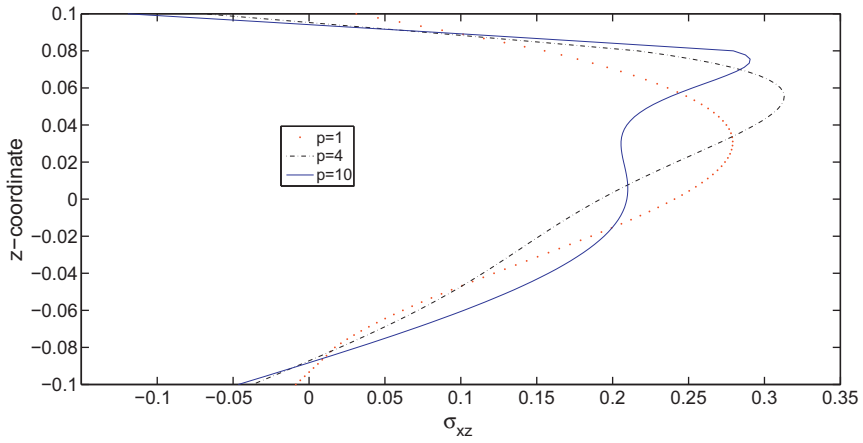

Fig. 12. Sandwich square plate with FGM core subjected to sinusoidal load at the top, with $a/h = 10$. σ_{xz} through the thickness direction at the point $(0, \frac{b}{2})$ for different values of p.

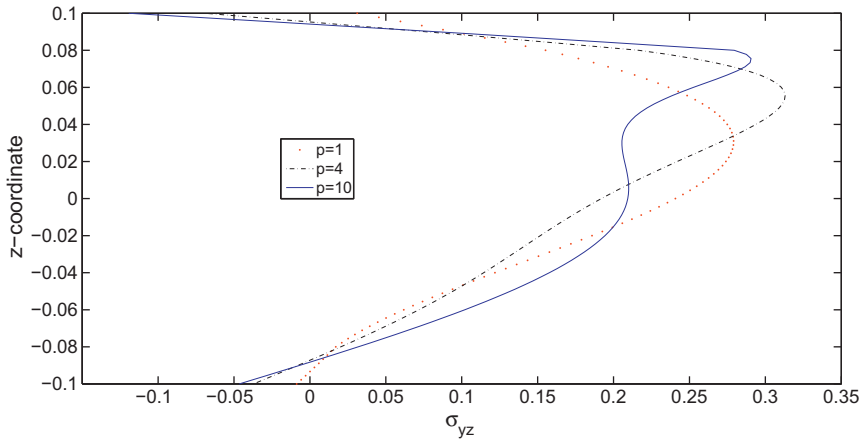

Fig. 13. Sandwich square plate with FGM core subjected to sinusoidal load at the top, with $a/h = 10$. σ_{yz} through the thickness direction at the point $(\frac{a}{2}, 0)$ for different values of p.

Table 5
Fundamental frequency $\bar{\omega} = \omega h\sqrt{\rho_m/E_m}$ of a SSSS isotropic functionally graded plate (Al/ZrO_2), $a/h = 5$, and using 13^2 points.

Source	$p = 2$	$p = 3$	$p = 5$
Ref. [8]	0.2153	0.2172	0.2194
Exact [29]	0.2197	0.2211	0.2225
Present, Sinus ($\epsilon_{zz} = 0$)	0.2189	0.2202	0.2215
Present, Sinus ($\epsilon_{zz} \neq 0$)	0.2198	0.2212	0.2225

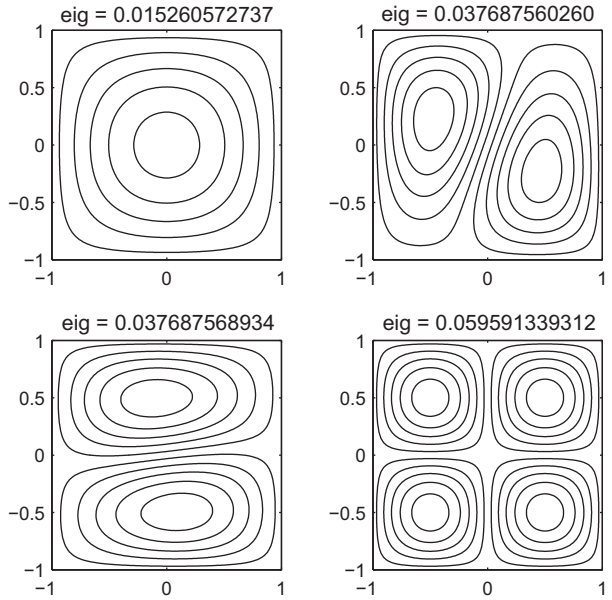

Fig. 14. First 4 frequencies $\bar{\omega} = \omega h\sqrt{\rho_m/E_m}$ of a SSSS isotropic functionally graded plate (Al/ZrO_2), with $a/h = 20$, $p = 1$, and using 17^2 points.

Table 6
First 10 frequencies $\bar{\omega} = \omega h\sqrt{\rho_m/E_m}$ of a SSSS isotropic functionally graded plate (Al/ZrO_2), $p = 1$.

$a/h = 20$				$a/h = 10$			
Present 13^2	17^2	21^2	Ref. [8]	13^2	17^2	21^2	Ref. [8]
0.0153	0.0153	0.0153	0.0149	0.0596	0.0596	0.0596	0.0584
0.0377	0.0377	0.0377	0.0377	0.1426	0.1426	0.1426	0.1410
0.0377	0.0377	0.0377	0.0377	0.1426	0.1426	0.1426	0.1410
0.0596	0.0596	0.0596	0.0593	0.2058	0.2058	0.2058	0.2058
0.0741	0.0739	0.0739	0.0747	0.2058	0.2058	0.2058	0.2058
0.0741	0.0739	0.0739	0.0747	0.2193	0.2193	0.2193	0.2164
0.0953	0.0950	0.0950	0.0769	0.2677	0.2676	0.2676	0.2646
0.0953	0.0950	0.0950	0.0912	0.2677	0.2676	0.2676	0.2677
0.1029	0.1029	0.1029	0.0913	0.2911	0.2910	0.2910	0.2913
0.1029	0.1029	0.1029	0.1029	0.3366	0.3363	0.3363	0.3264

5. Conclusions

A novel application of a unified formulation by a meshless discretization is proposed. A thickness-stretching sinusoidal shear deformation theory was implemented for the static and free vibration analysis of functionally graded plates.

The present formulation was compared with analytical, meshless or finite element methods and proved very accurate in both static and vibration problems. The effect of $\epsilon_{zz} \neq 0$ showed significance in thicker plates. Even for a thinner functionally graded plate, the σ_{zz} shoud always be considered in the formulation.

For the first time, the complete equations of motion and boundary conditions are present to help readers to implement it successfully with this or other strong-form techniques.

Appendix A. Fundamental nuclei

The stress–strain relations for functionally graded materials assume isotropic behavior at each layer k. Therefore, many terms are cancelled due to absence of membrane-bending coupling, etc. For a functionally graded plate the fundamental nuclei in explicit form are then obtained as:

$$\begin{aligned}
K^{k\tau s}_{uu_{11}} &= \left(-\partial^\tau_x\partial^s_x C_{11} + \partial^\tau_z\partial^s_z C_{55} - \partial^\tau_y\partial^s_y C_{66}\right)F_\tau F_s\\
K^{k\tau s}_{uu_{12}} &= \left(-\partial^\tau_x\partial^s_y C_{12} - \partial^\tau_y\partial^s_x C_{66}\right)F_\tau F_s\\
K^{k\tau s}_{uu_{13}} &= \left(-\partial^\tau_x\partial^s_z C_{13} + \partial^\tau_z\partial^s_x C_{55}\right)F_\tau F_s\\
K^{k\tau s}_{uu_{21}} &= \left(-\partial^\tau_y\partial^s_x C_{12} - \partial^\tau_x\partial^s_y C_{66}\right)F_\tau F_s\\
K^{k\tau s}_{uu_{22}} &= \left(-\partial^\tau_y\partial^s_y C_{22} + \partial^\tau_z\partial^s_z C_{44} - \partial^\tau_x\partial^s_x C_{66}\right)F_\tau F_s\\
K^{k\tau s}_{uu_{23}} &= \left(-\partial^\tau_y\partial^s_z C_{23} + \partial^\tau_z\partial^s_y C_{44}\right)F_\tau F_s\\
K^{k\tau s}_{uu_{31}} &= \left(\partial^\tau_z\partial^s_x C_{13} - \partial^\tau_x\partial^s_z C_{55}\right)F_\tau F_s\\
K^{k\tau s}_{uu_{32}} &= \left(\partial^\tau_z\partial^s_y C_{23} - \partial^\tau_y\partial^s_z C_{44}\right)F_\tau F_s\\
K^{k\tau s}_{uu_{33}} &= \left(\partial^\tau_z\partial^s_z C_{33} - \partial^\tau_y\partial^s_y C_{44} - \partial^\tau_x\partial^s_x C_{55}\right)F_\tau F_s
\end{aligned} \tag{A.1}$$

$$\begin{aligned}
\Pi^{k\tau s}_{11} &= \left(n_x\partial^s_x C_{11} + n_y\partial^s_y C_{66}\right)F_\tau F_s\\
\Pi^{k\tau s}_{12} &= \left(n_x\partial^s_y C_{12} + n_y\partial^s_x C_{66}\right)F_\tau F_s\\
\Pi^{k\tau s}_{13} &= n_x\partial^s_z C_{13}F_\tau F_s\\
\Pi^{k\tau s}_{21} &= \left(n_y\partial^s_x C_{12} + n_x\partial^s_y C_{66}\right)F_\tau F_s\\
\Pi^{k\tau s}_{22} &= \left(n_y\partial^s_y C_{22} + n_x\partial^s_x C_{66}\right)F_\tau F_s\\
\Pi^{k\tau s}_{23} &= n_y\partial^s_z C_{23}F_\tau F_s\\
\Pi^{k\tau s}_{31} &= n_x\partial^s_z C_{55}F_\tau F_s\\
\Pi^{k\tau s}_{32} &= n_y\partial^s_z C_{44}F_\tau F_s\\
\Pi^{k\tau s}_{33} &= \left(n_y\partial^s_y C_{44} + n_x\partial^s_x C_{55}\right)F_\tau F_s
\end{aligned} \tag{A.2}$$

References

[1] Miyamoto Y, Kaysser WA, Rabin BH, Kawasaki A, Ford RG. Functionally graded materials: design, processing and applications. Kluwer Academic Publishers; 1999.
[2] Zenkour AM. Generalized shear deformation theory for bending analysis of functionally graded plates. Appl Math Modell 2006;30.
[3] Cheng ZQ, Batra RC. Deflection relationships between the homogeneous kirchhoff plate theory and different functionally graded plate theories. Arch Mech 2000;52:143–58.
[4] Batra RC, Jin J. Natural frequencies of a functionally graded anisotropic rectangular plate. J Sound Vib 2005;282(1–2):509–16.
[5] Ferreira AJM, Batra RC, Roque CMC, Qian LF, Jorge RMN. Natural frequencies of functionally graded plates by a meshless method. Compos Struct 2006;75(1–4):593–600.
[6] Reddy JN. Analysis of functionally graded plates. Int J Numer Methods Eng 2000;47:663–84.
[7] Ferreira AJM, Batra RC, Roque CMC, Qian LF, Martins PALS. Static analysis of functionally graded plates using third-order shear deformation theory and a meshless method. Compos Struct 2005;69(4):449–57.
[8] Qian LF, Batra RC, Chen LM. Static and dynamic deformations of thick functionally graded elastic plate by using higher-order shear and normal deformable plate theory and meshless local Petrov-Galerkin method. Composites: Part B 2004;35:685–97.
[9] Carrera E, Brischetto S, Cinefra M, Soave M. Effects of thickness stretching in functionally graded plates and shells. Compos Part B: Engineering 2011;42:123–33.

[10] Kansa EJ. Multiquadrics – a scattered data approximation scheme with applications to computational fluid dynamics. I: surface approximations and partial derivative estimates. Comput Math Appl 1990;19(8/9):127–45.
[11] Ferreira AJM. A formulation of the multiquadric radial basis function method for the analysis of laminated composite plates. Compos Struct 2003;59:385–92.
[12] Ferreira AJM. Thick composite beam analysis using a global meshless approximation based on radial basis functions. Mech Adv Mater Struct 2003;10:271–84.
[13] Ferreira AJM, Roque CMC, Martins PALS. Analysis of composite plates using higher-order shear deformation theory and a finite point formulation based on the multiquadric radial basis function method. Composites: Part B 2003;34:627–36.
[14] Ferreira AJM, Roque CMC, Jorge RMN, Kansa EJ. Static deformations and vibration analysis of composite and sandwich plates using a layerwise theory and multiquadrics discretizations. Eng Anal Bound Elem 2005;29(12):1104–14.
[15] Ferreira AJM, Roque CMC, Jorge RMN. Analysis of composite plates by trigonometric shear deformation theory and multiquadrics. Comput Struct 2005;83(27):2225–37.
[16] Ferreira AJM, Batra RC, Roque CMC, Qian LF, Jorge RMN. Natural frequencies of functionally graded plates by a meshless method. Compos Struct 2006;75(1–4):593–600. Thirteenth International Conference on Composite Structures – ICCS/13.
[17] Ferreira AJM, Roque CMC, Jorge RMN. Free vibration analysis of symmetric laminated composite plates by fsdt and radial basis functions. Comput Methods Appl Mech Eng 2005;194(39–41):4265–78.
[18] Ferreira AJM, Roque CMC, Martins PALS. Radial basis functions and higher-order shear deformation theories in the analysis of laminated composite beams and plates. Compos Struct 2004;66(1–4):287–93. Twelfth International Conference on Composite Structures.
[19] Carrera E. C^0 Reissner–Mindlin multilayered plate elements including zig-zag and interlaminar stress continuity. Int J Numer Methods Eng 1996;39:1797–820.
[20] Carrera E. Developments, ideas, and evaluations based upon Reissner's mixed variational theorem in the modelling of multilayered plates and shells. Appl Mech Rev 2001;54:301–29.
[21] Touratier M. A generalization of shear deformation theories for axisymmetric multilayered shells. Int J Solids Struct 1992;29:1379–99.
[22] Touratier M. An efficient standard plate theory. Int J Eng Sci 1991;29:901–16.
[23] Touratier M. A refined theory of laminated shallow shells. Int J Solids Struct 1992;29(11):1401–15.
[24] Vidal P, Polit O. A family of sinus finite elements for the analysis of rectangular laminated beams. Compos Struct 2008;84:56–72.
[25] Neves AMA, Ferreira AJM, Carrera E, Roque CMC, Cinefra M, Jorge RMN, et al. Bending of fgm plates by a sinusoidal plate formulation and collocation with radial basis functions. Mech Res Commun, in press.
[26] Ferreira AJM, Fasshauer GE. Computation of natural frequencies of shear deformable beams and plates by a rbf-pseudospectral method. Comput Methods Appl Mech Eng 2006;196:134–46.
[27] Carrera E, Brischetto S, Robaldo A. Variable kinematic model for the analysis of functionally graded material plates. AIAA J 2008;46:194–203.
[28] Brischetto S. Classical and mixed advanced models for sandwich plates embedding functionally graded cores. J Mech Mater Struct 2009;4:13–33.
[29] Vel SS, Batra RC. Three-dimensional exact solution for the vibration of functionally graded rectangular plates. J Sound Vib 2004;272:703–30.